

# Filtering and Smoothing with Score-Driven Models\*

Giuseppe Buccheri<sup>1</sup>, Giacomo Bormetti<sup>2</sup>, Fulvio Corsi<sup>3,4</sup>, and Fabrizio Lillo<sup>2,5</sup>

<sup>1</sup>University of Rome Tor Vergata, Italy

<sup>2</sup>University of Bologna, Italy

<sup>3</sup>University of Pisa, Italy

<sup>4</sup>City University of London, UK

<sup>5</sup>CADS, Human Technopole, Milan, Italy

February 2021

## Abstract

We propose a methodology for filtering, smoothing and assessing parameter and filtering uncertainty in score-driven models. Our technique is based on a general representation of the Kalman filter and smoother recursions for linear Gaussian models in terms of the score of the conditional log-likelihood. We prove that, when data is generated by a nonlinear non-Gaussian state-space model, the proposed methodology results from a local expansion of the true filtering density. A formal characterization of the approximation error is provided. As shown in extensive Monte Carlo analyses, our methodology performs very similarly to exact simulation-based methods, while remaining computationally extremely simple. We illustrate empirically the advantages in employing score-driven models as approximate filters rather than purely predictive processes.

**Keywords:** State-Space models, Score-driven models, Kalman filter, Smoothing, Filtering uncertainty

**JEL codes:** C22, C32, C58.

---

\*Corresponding author: Giuseppe Buccheri, University of Rome Tor Vergata, Via Columbia 2, 00133 Roma (Italy). We are particularly grateful for suggestions we have received from Andrew Harvey, Marcin Zamojski and participants to the 11<sup>th</sup> CFE conference in London, the 11<sup>th</sup> SoFiE conference in Lugano, the 2018 IAAE conference in Montreal, the 2019 workshop on score-driven time-series models in Cambridge, the 2019 IAAE conference in Cyprus, the 6th RCEA Time Series Econometrics Workshop in Cyprus and the 2019 “Econometrics in The Areaa” workshop in Verona.

# 1 Introduction

GARCH-type models (Engle 1982, Bollerslev 1986) and, more generally, observation-driven models (Cox 1981), are a class of dynamic econometric models where time-varying parameters depend on past observations. When these models are regarded as data generating processes, the state variables are completely revealed by past observations, which thus encode all relevant information. As such, the only source of uncertainty affecting time-varying parameters is the finite sample distribution of the maximum likelihood estimator, known as *parameter uncertainty*. Since time-varying parameters are one-step-ahead predictable, observation-driven models can also be regarded as predictive filters. In this case, conditionally on past observations, the state variables have a non-degenerate density, which is known as *filtering uncertainty*. This implies that smoothing, i.e. using information from contemporaneous and future observations, provides better estimates compared to one-step-ahead predictions. Such idea was largely exploited by Daniel B. Nelson, who studied the properties of misspecified GARCH filters under the assumption that data is generated by a continuous-time diffusion<sup>1</sup>; see Nelson (1992), Nelson and Foster (1994), Nelson and Foster (1995) and Nelson (1996).

Despite the considerable amount of observation-driven models proposed in the literature, little attention has been paid to examine their properties as approximate filters for state-space models. We aim at partially filling this gap by introducing a filtering and smoothing methodology for a large subset of observation-driven models, the class of score-driven models of Creal et al. (2013) and Harvey (2013), also known as “Generalized Autoregressive Score” (GAS) models or “Dynamic Conditional Score” (DCS) models. In score-driven models, time-varying parameters are one-step-ahead predictable, with the normalized score of the conditional likelihood acting as a driving force. Since the score depends on the full shape of the observation density, the update of time-varying parameters is robust under non-normality; see also Harvey and Luati (2014). Few recent examples of applications of score-driven models in economics and finance are given by Oh and Patton (2017), Lucas et al. (2019), Babii et al. (2019), Linton and Wu (2020).

We show that the classical Kalman filter and smoother recursions for linear Gaussian models can be expressed solely in terms of the first and second derivatives of the conditional log-likelihood. In particular, the recursion of the predictive filter turns out to be an autoregressive process driven by the score. This result has two main implications. First, the recursions for linear Gaussian models can in principle be applied to nonlinear non-Gaussian models by replacing the Gaussian

---

<sup>1</sup>The interpretation of GARCH processes as predictive filters is well described in this statement by Nelson (1992): “Note that our use of the term ‘estimate’ corresponds to its use in the filtering literature rather than the statistics literature; that is, an ARCH model with (given) fixed parameters produces ‘estimates’ of the true underlying conditional covariance matrix at each point in time in the same sense that a Kalman filter produces ‘estimates’ of unobserved state variables in a linear system”.

score with the score of the non-Gaussian conditional density. When applied to nonlinear non-Gaussian models, these new recursions provide approximate estimates of the first two conditional moments of the state variables. The approximation is robust because the score accounts for the non-normality of the conditional density. Second, the analogy between the Kalman predictive filter and score-driven models allows to extend to score-driven filters the additional tools available for linear Gaussian models, namely: (i) the update filter, (ii) the smoother and (iii) the confidence bands around filtered and smoothed estimates. The update filter and the smoother improve over classical one-step-ahead predictions by exploiting the information of contemporaneous and future observations. The confidence bands account not only for parameter uncertainty, but even for filtering uncertainty, which is non-negligible if the model is employed as a filter.

The problem of filtering and smoothing for general state-space models reduces to a multi-dimensional integral which is often untreatable. Simulation-based techniques are typically employed to approximate such integrals. If data is generated by a nonlinear non-Gaussian state-space model, it becomes interesting to characterize the error made by replacing the optimal but computationally intensive filter with the approximate score-driven filter. We show that, under a specific normalization, score-driven filters result from a local expansion of the true filtering density around the special case in which state variables are non-stochastic. The error made in the expansion is characterized in detail, and it is shown to be proportional to the conditional variance and to a set of higher order moments of the state variables. This implies that the approximation is accurate whenever state variables do not change too much in time, whereas it is less precise if they have a large variance. The characterization of the approximation of score-driven filters sheds light on their relation with other approximate filtering methods which also employ the score, such as the filter of Masreliez (1975) and the approximation via mode estimation of Durbin and Koopman (2012).

The main advantage of the proposed methodology is that its computational complexity is the same as in linear Gaussian models. The predictive and update filters are computed iteratively through a forward recursion, whereas smoothing requires an additional backward recursion. The second conditional moments follow similar recursions. Despite its computational simplicity, the method provides very close results when compared to exact simulation-based methods. Our Monte-Carlo study shows that the average loss (in mean square error) imputable to the approximation is smaller than 2% for a wide range of scenarios. Computational times are instead much lower compared to exact methods. In the scenarios considered in the simulation study, we find that the average computational time needed for estimation, filtering and smoothing is between 150 and 800 times smaller compared to classical simulation methods based on importance sampling.

Our empirical study is devoted to highlight the advantages in employing score-driven models as approximate filters rather than purely predictive processes. Using data of stocks belonging to the US equity market, we show that the update filter and the smoother improve significantly over

classical one-step-ahead predictions. We also show that neglecting filtering uncertainty leads to a number of exceedances larger than expected when constructing confidence bands around filtered and smoothed estimates. Our results are tested using both univariate and multivariate stochastic volatility models. This is straightforward in our framework, as it remains computationally simple in high dimensions.

Beside the works of Nelson quoted above, observation-driven models have been regarded as approximate filters in other papers. Blasques et al. (2015) prove that score-driven filters are locally optimal based on information theoretic criteria; Koopman et al. (2016) show through an extensive Monte Carlo study that misspecified score-driven models provide similar forecasting performances as correctly specified parameter-driven models. Harvey (2013) proposes a related smoothing technique for a dynamic Student- $t$  location model by replacing the prediction error in the Kalman smoother recursions with the score of the Student- $t$  density. An application of such technique can be found in Caivano et al. (2016). Our approach is based on a representation of the Kalman filter and smoother recursions in terms of the score of the conditional log-likelihood which leads to different smoothing recursions. The latter are readily applicable to a general nonlinear non-Gaussian density.

The rest of the paper is organized as follows: Section (2) introduces the methodology, provides the main theoretical results and discusses the relation with other approximate filtering methods; Section (3) shows the results of the Monte Carlo study; in Section (4) the methodology is applied to a dataset of financial assets belonging to the Russel 3000 index; Section (5) concludes. The proofs of the main results are reported in the appendix.

## 2 Methodology

### 2.1 Linear Gaussian models

Our starting point is the classical theory of linear Gaussian models. Let us consider the following state-space representation:

$$\mathbf{y}_t = \mathbf{Z}\boldsymbol{\alpha}_t + \boldsymbol{\epsilon}_t, \quad \boldsymbol{\epsilon}_t \sim \text{NID}(\mathbf{0}, \mathbf{H}) \quad (2.1)$$

$$\boldsymbol{\alpha}_{t+1} = \mathbf{c} + \mathbf{T}\boldsymbol{\alpha}_t + \boldsymbol{\eta}_t, \quad \boldsymbol{\eta}_t \sim \text{NID}(\mathbf{0}, \mathbf{Q}) \quad (2.2)$$

where  $\boldsymbol{\alpha}_t \in \mathbb{R}^m$  is a vector of state variables and  $\mathbf{y}_t \in \mathbb{R}^p$  is a vector of observations. The parameters  $\mathbf{Z} \in \mathbb{R}^{p \times m}$ ,  $\mathbf{H} \in \mathbb{R}^{p \times p}$ ,  $\mathbf{T} \in \mathbb{R}^{m \times m}$  and  $\mathbf{Q} \in \mathbb{R}^{m \times m}$  are referred to as system matrices. The two errors  $\boldsymbol{\epsilon}_t$ ,  $\boldsymbol{\eta}_t$  are assumed to be normal, serially uncorrelated and mutually independent. Let  $\mathbf{Y}_t$  denote the set of observations up to time  $t$ , namely  $\mathbf{Y}_t = \{\mathbf{y}_1, \dots, \mathbf{y}_t\}$ . The objects of interest are the conditional mean and covariance of  $\boldsymbol{\alpha}_t$  given  $\mathbf{Y}_t$  (update step) and the conditional mean and

covariance of  $\boldsymbol{\alpha}_{t+1}$  given  $\mathbf{Y}_t$  (prediction step). We thus define:

$$\mathbf{a}_{t|t} = \mathbb{E}[\boldsymbol{\alpha}_t | \mathbf{Y}_t], \quad \mathbf{P}_{t|t} = \text{Var}[\boldsymbol{\alpha}_t | \mathbf{Y}_t] \quad (2.3)$$

$$\mathbf{a}_{t+1} = \mathbb{E}[\boldsymbol{\alpha}_{t+1} | \mathbf{Y}_t], \quad \mathbf{P}_{t+1} = \text{Var}[\boldsymbol{\alpha}_{t+1} | \mathbf{Y}_t] \quad (2.4)$$

The Kalman filter computes recursively  $\mathbf{a}_{t|t}$ ,  $\mathbf{P}_{t|t}$ ,  $\mathbf{a}_{t+1}$  and  $\mathbf{P}_{t+1}$ . Assuming  $\boldsymbol{\alpha}_1 \sim \mathcal{N}(\mathbf{a}_1, \mathbf{P}_1)$ , where  $\mathbf{a}_1$  and  $\mathbf{P}_1$  are known, for  $t = 2, \dots, n$ , we have (see e.g. Harvey 1991, Durbin and Koopman 2012):

$$\mathbf{v}_t = \mathbf{y}_t - \mathbf{Z}\mathbf{a}_t \quad (2.5)$$

$$\mathbf{a}_{t|t} = \mathbf{a}_t + \mathbf{P}_t \mathbf{Z}' \mathbf{F}_t^{-1} \mathbf{v}_t \quad (2.6)$$

$$\mathbf{a}_{t+1} = \mathbf{c} + \mathbf{T}\mathbf{a}_t + \mathbf{K}_t \mathbf{v}_t \quad (2.7)$$

and

$$\mathbf{F}_t = \mathbf{Z}\mathbf{P}_t \mathbf{Z}' + \mathbf{H} \quad (2.8)$$

$$\mathbf{P}_{t|t} = \mathbf{P}_t - \mathbf{P}_t \mathbf{Z}' \mathbf{F}_t^{-1} \mathbf{Z}\mathbf{P}_t \quad (2.9)$$

$$\mathbf{P}_{t+1} = \mathbf{T}\mathbf{P}_t (\mathbf{T} - \mathbf{K}_t \mathbf{Z})' + \mathbf{Q} \quad (2.10)$$

where  $\mathbf{K}_t = \mathbf{T}\mathbf{P}_t \mathbf{Z}' \mathbf{F}_t^{-1}$ . The conditional log-likelihood is normal, and can be computed as:

$$\log p(\mathbf{y}_t | \mathbf{Y}_{t-1}) = \text{const} - \frac{1}{2} (\log |\mathbf{F}_t| + \mathbf{v}_t' \mathbf{F}_t^{-1} \mathbf{v}_t) \quad (2.11)$$

The smoothed estimates  $\hat{\boldsymbol{\alpha}}_t = \mathbb{E}[\boldsymbol{\alpha}_t | \mathbf{Y}_n]$ ,  $\hat{\mathbf{P}}_t = \text{Var}[\boldsymbol{\alpha}_t | \mathbf{Y}_n]$ ,  $n \geq t$  can instead be computed through the following set of backward recursions:

$$\mathbf{r}_{t-1} = \mathbf{Z}' \mathbf{F}_t^{-1} \mathbf{v}_t + \mathbf{L}_t' \mathbf{r}_t \quad (2.12)$$

$$\hat{\boldsymbol{\alpha}}_t = \mathbf{a}_t + \mathbf{P}_t \mathbf{r}_{t-1} \quad (2.13)$$

and

$$\mathbf{N}_{t-1} = \mathbf{Z}' \mathbf{F}_t^{-1} \mathbf{Z} + \mathbf{L}_t' \mathbf{N}_t \mathbf{L}_t \quad (2.14)$$

$$\hat{\mathbf{P}}_t = \mathbf{P}_t - \mathbf{P}_t \mathbf{N}_{t-1} \mathbf{P}_t \quad (2.15)$$

where  $\mathbf{L}_t = \mathbf{T} - \mathbf{K}_t \mathbf{Z}$ ,  $\mathbf{r}_n = \mathbf{0}$ ,  $\mathbf{N}_n = \mathbf{0}$  and  $t = n, \dots, 1$ . The conditional distribution of  $\boldsymbol{\alpha}_t$  is normal with mean and covariance given by  $(\mathbf{a}_{t+1}, \mathbf{P}_{t+1})$ ,  $(\mathbf{a}_{t|t}, \mathbf{P}_{t|t})$ ,  $(\hat{\boldsymbol{\alpha}}_t, \hat{\mathbf{P}}_t)$ , depending on the conditioning set.

## 2.2 Approximate score-driven filtering and smoothing

Let us denote by  $\boldsymbol{\nabla}_t = \frac{\partial \log p(\mathbf{y}_t | \mathbf{Y}_{t-1})}{\partial \mathbf{a}_t}$  the score of the conditional log-likelihood<sup>2</sup> in Eq. (2.11) with respect to the predictive filter  $\mathbf{a}_t$ . From Eq. (2.11), it readily follows that in linear Gaussian models

<sup>2</sup>Note from Eq. (2.11) that  $\log p(\mathbf{y}_t | \mathbf{Y}_{t-1})$  depends on  $\mathbf{a}_t$  because  $\mathbf{v}_t$  does. In order to keep the notation simple, we avoid writing explicitly the dependence of  $p(\mathbf{y}_t | \mathbf{Y}_{t-1})$  on  $\mathbf{a}_t$ .

the score is given by:

$$\nabla_t = \mathbf{Z}'\mathbf{F}_t^{-1}\mathbf{v}_t \quad (2.16)$$

Let us also denote by  $\mathbf{H}_t$  the Hessian of the conditional log-likelihood, defined as the matrix of second partial derivatives of  $\log p(\mathbf{y}_t|\mathbf{Y}_{t-1})$  with respect to  $\mathbf{a}_t$ , namely  $\mathbf{H}_t^{(hk)} = \frac{\partial^2 \log p(\mathbf{y}_t|\mathbf{Y}_{t-1})}{\partial \mathbf{a}_t^{(h)} \partial \mathbf{a}_t^{(k)}}$ . In linear Gaussian models, we have:

$$\mathbf{H}_t = -\mathbf{Z}'\mathbf{F}_t^{-1}\mathbf{Z} \quad (2.17)$$

It is simple to re-write<sup>3</sup> the Kalman filter and smoother equations in terms of  $\nabla_t$  and  $\mathbf{H}_t$ . Indeed, Eq. (2.6), (2.7) become:

$$\mathbf{a}_{t|t} = \mathbf{a}_t + \mathbf{P}_t \nabla_t \quad (2.18)$$

$$\mathbf{a}_{t+1} = \mathbf{c} + \mathbf{T}\mathbf{a}_t + \mathbf{T}\mathbf{P}_t \nabla_t \quad (2.19)$$

whereas Eq. (2.9), (2.10) become:

$$\mathbf{P}_{t|t} = \mathbf{P}_t + \mathbf{P}_t \mathbf{H}_t \mathbf{P}_t \quad (2.20)$$

$$\mathbf{P}_{t+1} = \mathbf{T}\mathbf{P}_t(\mathbf{T} + \mathbf{T}\mathbf{P}_t \mathbf{H}_t)' + \mathbf{Q} \quad (2.21)$$

Similarly, the backward smoothing recursions (2.12)-(2.15) can be written as:

$$\mathbf{r}_{t-1} = \nabla_t + \mathbf{T}(\mathbf{I} + \mathbf{P}_t \mathbf{H}_t)\mathbf{r}_t \quad (2.22)$$

$$\hat{\boldsymbol{\alpha}}_t = \mathbf{a}_t + \mathbf{P}_t \mathbf{r}_{t-1} \quad (2.23)$$

and

$$\mathbf{N}_{t-1} = -\mathbf{H}_t + (\mathbf{I} + \mathbf{P}_t \mathbf{H}_t)' \mathbf{T}' \mathbf{H}_t \mathbf{T} (\mathbf{I} + \mathbf{P}_t \mathbf{H}_t) \quad (2.24)$$

$$\hat{\mathbf{P}}_t = \mathbf{P}_t - \mathbf{P}_t \mathbf{N}_{t-1} \mathbf{P}_t \quad (2.25)$$

where  $\mathbf{I}$  denotes the identity matrix.

Compared to the classical Kalman filter and smoother recursions shown in Section (2.1), the above equations only depend on the score and the Hessian matrix of the conditional density. This means that they can be applied given a general nonlinear non-Gaussian density  $p(\mathbf{y}_t|\mathbf{Y}_{t-1})$  depending on a set of time-varying parameters  $\mathbf{a}_t$ . More specifically, let us consider the following state-space model:

$$\mathbf{y}_t | \boldsymbol{\alpha}_t \sim p(\mathbf{y}_t | \boldsymbol{\alpha}_t) \quad (2.26)$$

$$\boldsymbol{\alpha}_{t+1} = \mathbf{c} + \mathbf{T}\boldsymbol{\alpha}_t + \boldsymbol{\eta}_t \quad (2.27)$$

---

<sup>3</sup>Since the expression of  $\mathbf{H}_t$  in Eq. (2.17) is independent from observations, it also coincides, up to the sign, with the conditional Fisher information matrix  $\mathbf{I}_t = \mathbb{E}[\nabla_t \nabla_t' | \mathbf{Y}_{t-1}]$ . However, this is a particular property of linear-Gaussian models which does not hold in general. To keep our formulation general, we re-write the recursions in terms of  $\mathbf{H}_t$  rather than  $\mathbf{I}_t$ . See also Theorem 2 in Section (2.3), which shows that the conditional covariance depends on the Hessian in nonlinear non-Gaussian models.

where  $E[\boldsymbol{\eta}_t] = 0$ ,  $\text{Var}[\boldsymbol{\eta}_t] = \mathbf{Q}$  and  $p(\mathbf{y}_t|\boldsymbol{\alpha}_t)$  is a known observation density. The process followed by  $\boldsymbol{\alpha}_{t+1}$  is the same as in Eq. (2.2), but we drop the normality assumption on  $\boldsymbol{\eta}_t$ . To obtain approximate first and second conditional moments of  $\boldsymbol{\alpha}_t$ , we can replace the Gaussian score in Eq. (2.16) with  $\frac{\partial \log p(\mathbf{y}_t|\mathbf{Y}_{t-1})}{\partial \mathbf{a}_t}$ , where  $p(\mathbf{y}_t|\mathbf{Y}_{t-1})$  is the conditional density of the model in Eq. (2.26), (2.27). This density is generally unknown in nonlinear non-Gaussian models. To run the recursions, we thus need to approximate  $p(\mathbf{y}_t|\mathbf{Y}_{t-1})$  with a known density  $\hat{p}(\mathbf{y}_t|\mathbf{Y}_{t-1})$ . Let  $p(\mathbf{y}_t|\boldsymbol{\alpha}_t)|_{\mathbf{a}_t}$  denote the value of  $p(\mathbf{y}_t|\boldsymbol{\alpha}_t)$  for  $\boldsymbol{\alpha}_t = \mathbf{a}_t$ . Proposition 1 in Section (2.3) provides a formal characterization of the error made by approximating  $p(\mathbf{y}_t|\mathbf{Y}_{t-1})$  with  $p(\mathbf{y}_t|\boldsymbol{\alpha}_t)|_{\mathbf{a}_t}$ . This result allows us to set the approximate density  $\hat{p}(\mathbf{y}_t|\mathbf{Y}_{t-1})$  as follows:

$$\hat{p}(\mathbf{y}_t|\mathbf{Y}_{t-1}) = p(\mathbf{y}_t|\boldsymbol{\alpha}_t)|_{\mathbf{a}_t} \quad (2.28)$$

Under this approximation, the conditional moments can be computed iteratively as in linear Gaussian models, and the approximation error can be accounted for through Proposition 1. We can also estimate the model parameters by maximizing the approximate log-likelihood function  $\log \hat{L} = \sum_{i=1}^n \log p(\mathbf{y}_i|\boldsymbol{\alpha}_i)|_{\mathbf{a}_i}$ . More generally, it will be shown in Section (2.3) that such filtering algorithm can be obtained by considering “small deviations” from a particular solution of the filtering problem, the one corresponding to setting  $\mathbf{Q} = \mathbf{0}$  in Eq. (2.27). This implies that the approximation is accurate whenever  $\boldsymbol{\alpha}_t$  does not change too much in time, whereas it is less precise when state variables have a large variance.

### 2.3 Characterizing the approximation error

We examine here in more detail the nature of the approximation made by the filtering algorithm proposed in Section (2.2). For simplicity, we restrict our attention to univariate models. Let us consider the univariate version of the state-space model in Eq. (2.26), (2.27):

$$y_t|\boldsymbol{\alpha}_t \sim p(y_t|\boldsymbol{\alpha}_t) \quad (2.29)$$

$$\boldsymbol{\alpha}_{t+1} = c + \phi\boldsymbol{\alpha}_t + \boldsymbol{\eta}_t \quad (2.30)$$

where  $|\phi| < 1$  and  $\boldsymbol{\eta}_t$  is a sequence of i.i.d. random variables with zero mean and variance  $q$ . Before showing the main results, we introduce the notation. The conditional density of  $\alpha_t$  given  $\alpha_{t-1}$  is indicated by  $p(\alpha_t|\alpha_{t-1})$ . Let us also denote by  $p(\alpha_t|Y_{t-1})$  the probability density of  $\alpha_t$  conditionally on observations up to time  $t-1$  and, similarly, by  $p(\alpha_t|Y_t)$  the probability density of  $\alpha_t$  conditionally on observations up to time  $t$ . The first raw moments of  $p(\alpha_t|Y_{t-1})$  and  $p(\alpha_t|Y_t)$  are indicated by  $a_t$  and  $a_{t|t}$ , respectively. We also denote by  $p_t$  the variance of  $p(\alpha_t|Y_{t-1})$  and by  $p_{t|t}$  the variance of  $p(\alpha_t|Y_t)$ . Finally, let  $\beta_t^{(j)}$ ,  $j > 1$ , denote the  $j$ -th absolute central moment of  $p(\alpha_t|Y_{t-1})$ , and let  $p_t^{(j)}$ ,  $j > 2$ , denote the  $j$ -th central moment of  $p(\alpha_t|Y_{t-1})$ . Hereafter,  $p(y_t|\boldsymbol{\alpha}_t)$  is regarded as a function of  $\boldsymbol{\alpha}_t$ , whereas the observations  $y_1, \dots, y_t$  are treated as being fixed.

We first provide the intuition behind our approximation technique. The filtering problem amounts to compute the integral of a given function of the state variables, say  $\mathcal{F}(\alpha_t)$ , over the posterior density  $p(\alpha_t|Y_t)$ . Using the Bayes rule, such integral can be written in the following general form:

$$\mathcal{G}(y_1, \dots, y_t) = N \int_{-\infty}^{+\infty} \mathcal{F}(\alpha_t) p(y_t|\alpha_t) p(\alpha_t|Y_{t-1}) d\alpha_t \quad (2.31)$$

where  $N$  is a normalization constant. If  $\mathcal{F}(\alpha_t) = 1$ , the function  $\mathcal{G}(y_1, \dots, y_t)$  corresponds to the predictive density  $p(y_t|Y_{t-1})$ ; if instead  $F(\alpha_t)$  is a power function, the integral coincides with the conditional moments of  $\alpha_t$ . For nonlinear non-Gaussian models, the filtering problem cannot be solved in closed form. Historically, the literature on approximate filtering has proposed several simplifying assumptions on the unknown density  $p(\alpha_t|Y_{t-1})$  in order to make the integral manageable, for instance assuming normality (Masreliez 1975), or considering Edgeworth, Gaussian sums or related polynomial expansions (Sorenson and Stubberud 1968, Sorenson and Alspach 1971).

To obtain a set of recursions similar to those appearing in Section (2.2), we follow a different route. We expand  $p(y_t|\alpha_t)$  up to a certain order in Taylor series in a neighborhood of the optimal filter  $a_t$ . By doing so, the function  $\mathcal{G}(y_1, \dots, y_t)$  in Eq. (2.31) reduces to a weighted sum of higher order moments, with weights given by the derivatives of  $p(y_t|\alpha_t)$  evaluated for  $\alpha_t = a_t$ . It thus shares the same structure of the recursions appearing in Section (2.2). Since we consider a local expansion around  $a_t$ , the approximation error is small when there is a large probability that  $\alpha_t$  is close to  $a_t$ , i.e. when  $p(\alpha_t|Y_{t-1})$  tends to a degenerate density. This is the case if  $\alpha_t$  is non-stochastic, which corresponds to setting the variance  $q$  of the innovations  $\eta_t$  in Eq. (2.30) equal to zero. In this particular case, filtering uncertainty vanishes and the approximation is exact. In the general case where  $\alpha_t$  is stochastic ( $q > 0$ ), there is a nonzero probability that  $\alpha_t$  is different from  $a_t$ , and thus the approximation error becomes non-negligible. As we will see in the following, the latter depends on the absolute central moments of  $p(\alpha_t|Y_{t-1})$ , which vanish when  $q$  goes to zero. Thus, if data is generated by a nonlinear non-Gaussian state-space model, the recursions of Section (2.2), which are derived by analogy with the Kalman filter, provide an accurate approximation to the true filtering density when state variables have a small variance<sup>4</sup>.

This technique can be regarded as a perturbation approach in the spirit of Fleming (1971). In other words, we consider a particular case in which the solution of the filtering problem is known, i.e. the case in which parameters are non-stochastic ( $q = 0$ ), and then compute an approximate solution of the general problem ( $q > 0$ ) by considering small deviations around this special case. See also

---

<sup>4</sup>An interesting case in which the approximation is accurate is the continuous-time infill asymptotic framework of Nelson (1992), in which the observations of an Ito diffusion are sampled more and more finely, and thus the variance of the underlying volatility process tends to zero. See also Buccheri et al. (2020), who investigate in simulations the performance of score-driven models as approximate filters for continuous-time processes in the infill asymptotic framework.



Komunjer and Sizova (2018), who use a related perturbation approach to recover an approximate filtering density in stochastic volatility models.

The approximation error can be formally characterized by making a set of regularity assumptions on  $p(y_t|\alpha_t)$  and on the rate with which the tails of  $p(\alpha_t|\alpha_{t-1})$  decay to zero. The latter assumption avoids that the remainder in the Taylor expansion diverges when integrating out over  $p(\alpha_t|Y_{t-1})$ , and at the same time guarantees the existence of the conditional moments appearing in the recursions. We start by approximating the predictive density  $p(y_t|Y_{t-1})$ , i.e. we set  $\mathcal{F}(\alpha_t) = 1$  in Eq. (2.31). The following assumptions on  $p(y_t|\alpha_t)$  and  $p(\alpha_t|\alpha_{t-1})$  are made:

**Assumption 1.** *The observation density  $p(y_t|\alpha_t)$  is a bounded function of  $\alpha_t$ , twice differentiable in  $\mathbb{R}$  with continuous second derivative.*

**Assumption 2.** *For all  $b \in \mathbb{R}$ , there exists  $\bar{\delta} > 0$  such that  $p(\alpha_t|\alpha_{t-1}) < \frac{1}{|\alpha_t - b|^{3+\beta}}$ ,  $\beta > 0$ , for all  $\alpha_t$  such that  $|\alpha_t - b| > \bar{\delta}$  and for all  $\alpha_{t-1} \in \mathbb{R}$ .*

Assumption 1 implicitly requires that  $p(y_t|\alpha_t)$  is defined for any  $\alpha_t \in \mathbb{R}$ . This condition is not restrictive because, if  $\alpha_t \in \mathcal{C} \subset \mathbb{R}$  is bounded, it can always be transformed into an unbounded variable through an appropriate link function  $f : \mathcal{C} \rightarrow \mathbb{R}$ . The condition in Assumption 2 allows the density of the innovations  $\eta_t$  in Eq. (2.30) being non-normal, however it restricts its tails to decay faster than a certain power of  $\alpha_t$ . Lemma 1 in the appendix implies that such condition guarantees the existence of the second conditional moment of  $p(\alpha_t|Y_{t-1})$ . As shown in appendix A, the following result holds:

**Proposition 1.** *Let Assumptions 1,2 hold. Then, for any  $\gamma > 0$ , we can find  $\tilde{\delta} > \bar{\delta}$  such that:*

$$p(y_t|Y_{t-1}) = p(y_t|\alpha_t)|_{a_t} + \xi_t \tag{2.32}$$

with  $|\xi_t| < \gamma + \frac{1}{2} \sup_{|\alpha_t - a_t| < \tilde{\delta}} \left| \frac{\partial^2 p(y_t|\alpha_t)}{\partial \alpha_t^2} \right| p_t$ .

This result characterizes the error made by replacing the true conditional density  $p(y_t|Y_{t-1})$  by the approximate density  $p(y_t|\alpha_t)|_{a_t}$  in the filtering algorithm of Section (2.2); see Eq. (2.28). The error includes a component which can be made arbitrarily small, and an additional term which is zero only if  $p_t = 0$ , which is the case if  $q$  is equal to zero<sup>5</sup>. In this particular case,  $y_t$  is independent from past observations and  $p(y_t|Y_{t-1})$  naturally coincides with the marginal density of  $y_t$ . If  $q$  is nonzero, the second component of the error depends on  $p_t$  and the absolute second derivative of  $p(y_t|\alpha_t)$  in a neighborhood of  $a_t$ . In particular, as  $p_t$  is a monotonically increasing function of  $q$ , the error will increase with increasing  $q$ .

---

<sup>5</sup>Note that the condition  $p_t = 0$  is equivalent to the condition  $q = 0$ . Indeed, if  $q = 0$ , then  $p_t = 0$  by the law of total variance. If instead  $p_t = 0$ , then the relation  $p_t = \phi^2 p_{t-1|t-1} + q$  implies  $p_{t-1|t-1} = 0$  and  $q = 0$ , since both quantities are larger or equal than zero by definition.

We now consider the case  $\mathcal{F}(\alpha_t) = \alpha_t$ , which provides the conditional mean of  $\alpha_t$ . Compared to the previous case, the degree of the polynomial appearing inside the integral in Eq. (2.31) increases by one. To avoid that the approximation error diverges, we thus need a more restrictive condition on the tails of  $p(\alpha_t|\alpha_{t-1})$ :

**Assumption 3.** *For all  $b \in \mathbb{R}$ , there exists  $\bar{\delta} > 0$  such that  $p(\alpha_t|\alpha_{t-1}) < \frac{1}{|\alpha_t - b|^{4+\beta}}$ ,  $\beta > 0$ , for all  $\alpha_t$  such that  $|\alpha_t - b| > \bar{\delta}$  and for all  $\alpha_{t-1} \in \mathbb{R}$ .*

Note that, by virtue of Lemma 1 in the appendix, the above assumption implies the existence of the conditional moments of  $p(\alpha_t|Y_{t-1})$  up to the third order. In particular, Assumption 3 implies Assumption 2, so that if Assumptions 1 and 3 are satisfied, Proposition 1 holds. Let us denote by  $\nabla_t$  the score of the conditional density  $p(y_t|\alpha_t)$  computed for  $\alpha_t = a_t$ , namely

$$\nabla_t = \left. \frac{\partial \log p(y_t|\alpha_t)}{\partial \alpha_t} \right|_{a_t} \quad (2.33)$$

In appendix B, we prove the following theorem:

**Theorem 1.** *Let Assumptions 1,3 hold. Then, for any  $\gamma > 0$ , we can find  $\tilde{\delta} > \bar{\delta}$  such that:*

$$a_{t|t} = a_t + p_t \nabla_t + \chi_t + O(\xi_t) \quad (2.34)$$

where  $|\chi_t| < \gamma + \frac{1}{2p(y_t|\alpha_t)|_{a_t}} \sup_{|\alpha_t - a_t| < \tilde{\delta}} \left| \frac{\partial^2 p(y_t|\alpha_t)}{\partial \alpha_t^2} \right| \left( \beta_t^{(3)} + |a_t| p_t \right)$  and  $O(\xi_t)$  denotes terms of order  $\xi_t$ .

This result states that the approximate update filter  $a_t + p_t \nabla_t$  in Eq. (2.18) differs from the optimal update filter  $a_{t|t}$  because of two terms. The first term is the error  $\chi_t$  arising upon integrating the remainder in the series expansion of  $p(y_t|\alpha_t)$  over the posterior density  $p(\alpha_t|Y_{t-1})$ . Similarly to the approximation error  $\xi_t$  in Proposition 1, it increases with increasing  $q$  and tends to zero when  $q$  becomes small. Note however that the magnitude of  $\chi_t$  is related not only to  $p_t$ , but even to the third absolute central moment  $\beta_t^{(3)}$ . The second error term is of order  $\xi_t$ , and thus it also tends to zero when  $q$  becomes small.

Combining the result in Theorem 1 with Eq. (2.30), it is simple to obtain a recursive formula for the predictive filter  $a_t$ . Indeed, under the same assumptions of Theorem 1, we have:

$$a_{t+1} = c + \phi a_t + \phi p_t \nabla_t + \phi \chi_t + O(\xi_t) \quad (2.35)$$

which coincides with the approximate predictive filter in Eq. (2.19) up to the two error terms.

To compute  $p_{t|t}$ , we set  $\mathcal{F}(\alpha_t) = (\alpha_t - a_{t|t})^2$  in Eq. (2.31) and make the following two assumptions:

**Assumption 4.** *The observation density  $p(y_t|\alpha_t)$  is a bounded function of  $\alpha_t$ , three times differentiable in  $\mathbb{R}$  with continuous third derivative.*

**Assumption 5.** For all  $b \in \mathbb{R}$ , there exists  $\bar{\delta} > 0$  such that  $p(\alpha_t|\alpha_{t-1}) < \frac{1}{|\alpha_t - b|^{6+\beta}}$ ,  $\beta > 0$ , for all  $\alpha_t$  such that  $|\alpha_t - b| > \bar{\delta}$  and for all  $\alpha_{t-1} \in \mathbb{R}$ .

Assumption 4 implies a higher degree of smoothness for  $p(y_t|\alpha_t)$ . The main reason is that, in order to recover an expression similar to that in Eq. (2.20), we need a second order polynomial in the Taylor expansion. Assumption 5 is more restrictive than Assumption 3 because the degree of the polynomial inside the integral in Eq. (2.31) is now higher. Let  $h_t$  denote the Hessian of the conditional log-density  $p(y_t|\alpha_t)$  evaluated for  $\alpha_t = a_t$ , namely

$$h_t = \left. \frac{\partial^2 \log p(y_t|\alpha_t)}{\partial \alpha_t^2} \right|_{a_t}$$

The following theorem is proved in appendix C:

**Theorem 2.** Let Assumptions 4,5 hold. Then, for any  $\gamma > 0$ , we can find  $\tilde{\delta} > \bar{\delta}$  such that:

$$p_{t|t} = p_t + p_t^2 h_t + \ell_t + \zeta_t + O(\xi_t) + O(\chi_t) \quad (2.36)$$

where  $\ell_t = \nabla_t p_t^{(3)} + \frac{1}{2p(y_t|\alpha_t)|_{a_t}} \frac{\partial^2 p(y_t|\alpha_t)}{\partial \alpha_t^2} \Big|_{a_t} \left( p_t^{(4)} - 2p_t^2 \right)$ ,  $|\zeta_t| < \gamma + \frac{1}{6p(y_t|\alpha_t)|_{a_t}} \sup_{|\alpha_t - a_t| < \tilde{\delta}} \left| \frac{\partial^3 p(y_t|\alpha_t)}{\partial \alpha_t^3} \right| \beta_t^{(5)}$  and  $O(\xi_t)$ ,  $O(\chi_t)$  denote terms of order  $\xi_t$ ,  $\chi_t$ , respectively.

Eq. (2.36) characterizes the error made in Eq. (2.20) by approximating  $p_{t|t}$  with  $p_t + p_t^2 h_t$ . Together with the term  $\zeta_t$  arising from the integration of the reminder in the Taylor expansion, we have the additional error  $\ell_t$  which depends on the third and fourth conditional moments. This term does not appear in Eq. (2.20) because the latter is derived by analogy with linear Gaussian models in which the conditional second moment does not depend on higher order moments.

More generally, if we compute the conditional moments up to the  $k$ -th order, the  $k$ -th moment will depend on the  $(k+1)$ -th moment if a first-order Taylor expansion is considered (as in Theorem 1), and on the  $(k+1)$  and  $(k+2)$ -th moments if a second-order expansion is performed (as in Theorem 2). Similarly, the magnitude of the error arising from the reminder in the Taylor expansion will depend on the  $(k+2)$ -th absolute central moment in the case of a first order expansion, and on the  $(k+3)$ -th absolute central moment in the case of a second order expansion. Note that, using this method, it is possible to introduce approximate filtering algorithms which extend the one proposed in Section (2.2). An improved algorithm would include the extra terms arising from a higher order expansion and the computation of higher order conditional moments. Such algorithm would lead to an update mechanism for the predictive filter different from Eq. (2.19), which is of similar form as in score-driven models. As we are interested in studying the filtering problem within this class of models, we consider here with the recursions of Section (2.2), leaving the development of a more general filtering algorithm as a future work.

We conclude this section by observing that the result in Theorem 2 can be combined with Eq. (2.30) to obtain an expression for  $p_t$ . Under the same assumptions of Theorem 2, we have:

$$p_{t+1} = \phi^2(p_t + p_t^2 h_t) + q + \phi^2 \ell_t + \phi^2 \zeta_t + O(\xi_t) + O(\chi_t) \quad (2.37)$$

which characterizes the error made in Eq. (2.21) by replacing  $p_{t+1}$  with  $\phi^2(p_t + p_t^2 h_t) + q$ .

## 2.4 Relation with observation-driven models

The predictive filter in Eq. (2.19) belongs to the class of score-driven models of Creal et al. (2013) and Harvey (2013). Specifically, in score-driven models, the vector of time-varying parameters  $\mathbf{a}_t$  evolves as:

$$\mathbf{a}_{t+1} = \mathbf{c} + \mathbf{T}\mathbf{a}_t + \mathbf{A}\mathbf{S}_t\boldsymbol{\nabla}_t \quad (2.38)$$

where  $\mathbf{S}_t$  is a normalization matrix that accounts for the curvature of the conditional log-likelihood. The update in Eq. (2.19) is obtained by setting  $\mathbf{S}_t = \mathbf{A}^{-1}\mathbf{T}\mathbf{P}_t$  and letting  $\mathbf{P}_t$  evolve based on Eq. (2.21). The representation in Eq. (2.19) picks up a particular normalization that is analogous to the one used in the Kalman filter. Compared to the typical normalization adopted in score-driven models, based on inverse powers of the Fisher information, this normalization has two interesting features. First, the fact that the second conditional moments are independent from observations is a particular property of linear Gaussian models which does not hold in general; see Anderson and Moore (1979). It is thus natural that the covariance matrix  $\mathbf{P}_t$  depends on the Hessian, which generally depends on observations in nonlinear non-Gaussian models. Second, the static parameters appearing in Eq. (2.19) and (2.21), namely the system matrices  $\mathbf{c}$ ,  $\mathbf{T}$  and  $\mathbf{Q}$ , have an immediate interpretation, as they are the same parameters appearing in the state-space model in Eq. (2.29), (2.30). This one-to-one correspondence between the parameters of the underlying state-space model and the parameters of the approximate filter fails to hold under different normalization schemes.

When the normalization matrix  $\mathbf{S}_t$  is set differently, the conditional covariance  $\mathbf{P}_t$  can be defined by analogy with the recursions in Section (2.2). Specifically, observe that Eq. (2.19) coincides with Eq. (2.38) upon re-defining the conditional covariance matrix as  $\mathbf{P}_t = \mathbf{T}^{-1}\mathbf{A}\mathbf{S}_t$ . Thus, we can still apply the approximate recursions of Section (2.2) provided that the matrix  $\mathbf{P}_t$  is replaced by  $\mathbf{T}^{-1}\mathbf{A}\mathbf{S}_t$ ; see also appendix D, which describes in detail the filtering algorithm under a generic normalization matrix  $\mathbf{S}_t$ . The Monte-Carlo analysis of Section (3) compares the normalization of Section (2.2) with the classical normalization adopted in score-driven models, and finds that the difference between the two implementations is generally small. However, we point out that the use of the particular normalization given by Eq. (2.21) is essential when dealing with models with a number of latent components larger than the number of signals, i.e. when  $m > p$ . In this case, defining the conditional covariance as  $\mathbf{P}_t = \mathbf{T}^{-1}\mathbf{A}\mathbf{S}_t$  may not be enough to uniquely identify<sup>6</sup> the matrix  $\mathbf{A}$ . We provide more details on this point in appendix E.

Preferring one or another scaling method depends on the specific problem at hand. If one aims to compute smoothed estimates and/or confidence bands of standard score-driven models

---

<sup>6</sup>We thank Andrew Harvey for pointing this out.

employing a specific normalization  $\mathbf{S}_t$ , then it is convenient to compute  $\mathbf{P}_t$  as  $\mathbf{T}^{-1}\mathbf{A}\mathbf{S}_t$  and using the recursions of Appendix D. If in contrast one is not bound to the use of a specific normalization, and/or if the signal has more latent components, then it is convenient to adopt the normalization of Eq. (2.21), which allows to formally characterize the approximation error and uniquely identify  $\mathbf{P}_t$ .

## 2.5 Relation with other approximate filtering methods

Several filtering algorithms based on the score have been proposed in the literature. These algorithms arise from approximations to the true posterior density which are fundamentally different from the power series expansion shown here. Consequently, they lead to different expressions for the approximate conditional moments.

One example is given by the robust filter of Masreliez (1975), which assumes that the posterior density  $p(\boldsymbol{\alpha}_t|\mathbf{Y}_{t-1})$  is Gaussian. Under such assumption, the approximate conditional density  $\hat{p}(\mathbf{y}_t|\mathbf{Y}_{t-1})$  is given by:

$$\hat{p}(\mathbf{y}_t|\mathbf{Y}_{t-1}) = \int_{\mathbb{R}^m} p(\mathbf{y}_t|\boldsymbol{\alpha}_t)\hat{p}(\boldsymbol{\alpha}_t|\mathbf{Y}_{t-1})d\boldsymbol{\alpha}_t \quad (2.39)$$

where  $\hat{p}(\boldsymbol{\alpha}_t|\mathbf{Y}_{t-1})$  is Gaussian. Evaluating  $p(\mathbf{y}_t|\mathbf{Y}_{t-1})$  thus requires the computation of the convolution in Eq. (2.39), which differs from the simple approximate conditional density  $p(\mathbf{y}_t|\boldsymbol{\alpha}_t)|_{\mathbf{a}_t}$  in Eq. (2.28). The first and second conditional moments depend on the score and the Hessian matrix, however they are computed with respect to the more complicated density in Eq. (2.39). It is also not clear how the approximation error made by replacing  $p(\boldsymbol{\alpha}_t|\mathbf{Y}_{t-1})$  with a Gaussian density can be formally characterized.

The proposed method is also related to the class of approximating linear Gaussian models proposed by Durbin and Koopman (1997) and Durbin and Koopman (2012) to set the parameters of the density used in the importance sampling method for nonlinear non-Gaussian models. These authors construct a sequence of linear Gaussian models that approximate the nonlinear non-Gaussian model in a neighborhood of the conditional mode. The approximating linear Gaussian model at the  $j$ -th iteration has the form of Eq. (2.1), (2.2), with  $\mathbf{y}_t$  replaced by:

$$\tilde{\mathbf{y}}_t^{(j)} = \mathbf{Z}\tilde{\boldsymbol{\alpha}}_t^{(j-1)} - \ddot{\mathbf{h}}_t^{(j)-1}\dot{\mathbf{h}}_t^{(j)} \quad (2.40)$$

where

$$\dot{\mathbf{h}}_t^{(j)} = -\frac{\partial \log p(\mathbf{y}_t|\boldsymbol{\alpha}_t)}{\partial \boldsymbol{\alpha}_t} \Big|_{\tilde{\boldsymbol{\alpha}}_t^{(j-1)}}, \quad \ddot{\mathbf{h}}_t^{(j)} = -\frac{\partial^2 \log p(\mathbf{y}_t|\boldsymbol{\alpha}_t)}{\partial \boldsymbol{\alpha}_t \partial \boldsymbol{\alpha}_t'} \Big|_{\tilde{\boldsymbol{\alpha}}_t^{(j-1)}} \quad (2.41)$$

and the matrix  $\mathbf{H}$  replaced by  $\tilde{\mathbf{H}}_t^{(j)} = \ddot{\mathbf{h}}_t^{(j)-1}$  at each time-step. Here,  $\tilde{\boldsymbol{\alpha}}_t^{(j-1)}$  denotes the smoothed estimate obtained from the previous iteration of the Kalman filter and smoother recursions, whereas  $p(\mathbf{y}_t|\boldsymbol{\alpha}_t)$  denotes the observation density of the nonlinear non-Gaussian model. The method proceeds iteratively by running new Kalman filter and smoother recursions with  $\tilde{\mathbf{H}}_t^{(j)}$  and  $\tilde{\mathbf{y}}_t^{(j)}$  as

an input. Shephard and Pitt (1997) recover the same approximation although using a different approach.

Even in this method, the approximate recursions are driven by the score and the Hessian of the conditional density. However, the latter are evaluated using the trial value  $\tilde{\boldsymbol{\alpha}}_t^{(j-1)}$  recovered from the previous run of the Kalman filter and smoother. As such, the update of time-varying parameters in the mode approximation technique is not the same as in observation-driven models. Rather, each run of the Kalman filter and smoother can be seen as an iteration of a Newton-Raphson method in the space spanned by the state-variables, as formally shown by Durbin and Koopman (2012).

Harvey (2013) proposes a smoother for score-driven models by replacing the prediction error in the Kalman smoother for linear Gaussian models with the score of the conditional likelihood. This leads to smoother recursions which are different from the ones in Section (2.2), as can be verified by substituting repeatedly  $\mathbf{r}_t$  in Eq. (2.22) and comparing the resulting exponential decay of smoother weights with that of Harvey (2013).

## 2.6 Parameter and filtering uncertainty

The recursions in Eq. (2.19)-(2.21) provide approximate estimates of the first two conditional moments of the state variables. Confidence bands around filtered and smoothed estimates can be constructed either by exploiting the Chebyshev's inequality, or by computing the quantiles of a normal distribution with mean and variance given by the approximate filtering algorithm.

Built in this way, confidence bands would neglect parameter uncertainty, because the conditional moments are computed conditionally on static parameters. In order to also account for parameter uncertainty, we follow the approach usually adopted in linear Gaussian models. Specifically, we adopt the Bayesian perspective that the vector of static parameters, that we denote by  $\boldsymbol{\theta}$ , is a random variable with a certain prior distribution  $p(\boldsymbol{\theta})$ . In practice,  $p(\boldsymbol{\theta})$  can be set equal to the asymptotic distribution of the maximum likelihood estimate  $\hat{\boldsymbol{\theta}}$ , as in Blasques et al. (2016). Let  $\mathbf{a}_t^{\hat{\boldsymbol{\theta}}}$  denote the predictive filter computed from  $\hat{\boldsymbol{\theta}}$ . It is possible to show (Hamilton 1986) that the total conditional variance can be decomposed into the sum of two terms:

$$\begin{aligned} & \text{E}[(\boldsymbol{\alpha}_t - \mathbf{a}_t^{\hat{\boldsymbol{\theta}}})(\boldsymbol{\alpha}_t - \mathbf{a}_t^{\hat{\boldsymbol{\theta}}})' | \mathbf{Y}_{t-1}] = \\ & \text{E}_{\boldsymbol{\theta}}[(\boldsymbol{\alpha}_t - \mathbf{a}_t^{\boldsymbol{\theta}})(\boldsymbol{\alpha}_t - \mathbf{a}_t^{\boldsymbol{\theta}})' | \mathbf{Y}_{t-1}] + \text{E}_{\boldsymbol{\theta}}[(\mathbf{a}_t^{\boldsymbol{\theta}} - \mathbf{a}_t^{\hat{\boldsymbol{\theta}}})(\mathbf{a}_t^{\boldsymbol{\theta}} - \mathbf{a}_t^{\hat{\boldsymbol{\theta}}})'] = \\ & \text{E}_{\boldsymbol{\theta}}[\mathbf{P}_t^{\boldsymbol{\theta}}] + \text{E}_{\boldsymbol{\theta}}[(\mathbf{a}_t^{\boldsymbol{\theta}} - \mathbf{a}_t^{\hat{\boldsymbol{\theta}}})(\mathbf{a}_t^{\boldsymbol{\theta}} - \mathbf{a}_t^{\hat{\boldsymbol{\theta}}})'] \end{aligned} \quad (2.42)$$

where  $\text{E}_{\boldsymbol{\theta}}[\cdot]$  denotes the expectation taken with respect to the prior density  $p(\boldsymbol{\theta})$ . The first term is related to filtering uncertainty. It represents the conditional variance of the state variables averaged over the density  $p(\boldsymbol{\theta})$ . The second term is instead related to parameter uncertainty, as it represents the variance of  $\mathbf{a}_t^{\boldsymbol{\theta}}$  due to the randomness of  $\boldsymbol{\theta}$  around its maximum likelihood estimate  $\hat{\boldsymbol{\theta}}$ . Both terms can be computed by simulations, sampling from the prior density  $p(\boldsymbol{\theta})$  and computing the

sample mean. The Monte Carlo analysis in Section (3) shows that the such methodology provides an accurate matching between the nominal confidence level and the average coverage of the bands.

### 3 Monte Carlo analysis

In this section we aim to examine by Monte-Carlo simulations the performance of the approximate filtering and smoothing algorithm of Section (2.2). The main idea is to assess the loss incurred by the approximation through a comparison with an exact simulation-based method. As a data generating process, we consider several nonlinear non-Gaussian state-space models having the form of Eq. (2.29), (2.30). In particular, we specify the observation density in Eq. (2.29) as follows:

$$\begin{aligned}
 \text{Location (Student-}t\text{):} & & y_t &= \alpha_t + \epsilon_t, & \epsilon_t &\sim t_\nu(0, e^\lambda) \\
 \text{Scale (Gaussian):} & & y_t &= e^{\frac{\alpha_t}{2}} \epsilon_t, & \epsilon_t &\sim N(0, 1) \\
 \text{Scale (Student-}t\text{):} & & y_t &= e^{\frac{\alpha_t}{2}} \epsilon_t, & \epsilon_t &\sim t_\nu(0, 1) \\
 \text{Count data (Poisson):} & & y_t &\sim \text{Poiss}(\alpha_t)
 \end{aligned}$$

where the state variable  $\alpha_t$  evolves according to the process in Eq. (2.30):

$$\alpha_{t+1} = c + \phi\alpha_t + \eta_t, \quad \eta_t \sim N(0, q) \quad (3.1)$$

For simplicity, we assume here that  $\eta_t$  are normal innovations<sup>7</sup>. However, the results of Section (2.3) show that the approximation error remains bounded even in the presence of fat-tailed densities; see Assumptions 2, 3 and 5 of Section (2.3). The variance  $q$  is an important parameter because it is related to the accuracy of the approximation. Based on the results of Section (2.3), the approximation error is small whenever  $q$  is close to zero, and tends to increase with  $q$ . The performance of the approximate algorithm is thus examined for increasing values of  $q$ . In particular, we consider three scenarios with  $q = 0.005$ ,  $q = 0.01$  and  $q = 0.05$ . The other static parameters in Eq. (3.1) are set as  $c = 0.001$  and  $\phi = 0.98$ . The noise log-variance parameter in the location model is set as  $\lambda = \log(5q)$ , which restricts the noise-to-signal ratio  $e^\lambda/q$  to be equal to 5 in each scenario. We discuss later the effect, on the obtained results, of choosing a different value for the noise-to-signal ratio. Finally, the degrees of freedom parameter in the two models based on the Student- $t$  density is set as  $\nu = 3$ .

Optimal filtered and smoothed estimates of  $\alpha_t$  are computed using Importance Sampling (IS), as described e.g. by Durbin and Koopman (2012). To set the importance density, we use the ‘‘Numerically Accelerated Importance Sampling’’ (NAIS) method of Koopman et al. (2015), implemented by sampling  $N = 400$  antithetic paths of  $\alpha_t$  from the importance density. The IS filtered

---

<sup>7</sup>This assumption simplifies the implementation of the importance sampling algorithm used to compute the optimal filtered and smoothed estimates. See also Koopman et al. (2016), who perform a similar Monte-Carlo study.

Model	Distribution	$\hat{p}(y_t Y_{t-1}) = p(y_t \alpha_t) _{a_t}$	Normalization $\mathbf{S}_t$
Location	Student- $t$	$\frac{\Gamma(\frac{\nu+1}{2})}{\Gamma(\frac{\nu}{2})\sqrt{\pi(\nu-2)}e^\lambda} \left(1 + \frac{(y_t - a_t)^2}{(\nu-2)e^\lambda}\right)^{-\frac{\nu+1}{2}}$	$\frac{\nu}{\nu+1}e^{2\lambda}$
Scale	Gaussian	$\frac{1}{\sqrt{2\pi}e^{a_t}} \exp\left(-\frac{y_t^2}{2e^{a_t}}\right)$	1
Scale	Student- $t$	$\frac{\Gamma(\frac{\nu+1}{2})}{\Gamma(\frac{\nu}{2})\sqrt{\pi(\nu-2)}e^{a_t}} \left(1 + \frac{y_t^2}{(\nu-2)e^{a_t}}\right)^{-\frac{\nu+1}{2}}$	1
Count data	Poisson	$\frac{a_t^{y_t} e^{-a_t}}{y_t!}$	$e^{-a_t}$

**Table 1:** For each state-space model, we specify the approximate conditional density  $\hat{p}(y_t|Y_{t-1}) = p(y_t|\alpha_t)|_{a_t}$  in the filtering algorithm of Section (2.2), and the normalization  $\mathbf{S}_t$  used in the observation-driven model.

and smoothed estimates are computed after estimating the static parameters of the four state-space models using the same NAIS algorithm. As a further benchmark, we examine the performance of the standard Kalman filter in the location model, and the QMLE method of Harvey et al. (1994) in the two stochastic volatility models.

Table (1) reports, for each state-space model, the specific expression of the approximate predictive density  $\hat{p}(y_t|Y_{t-1}) = p(y_t|\alpha_t)|_{a_t}$  in the filtering and smoothing algorithm of Section (2.2). We implement this algorithm using both the normalization in Eq. (2.21), for which the results of Section (2.3) hold, and the classical normalization  $\mathbf{S}_t$  adopted in the literature on score-driven models<sup>8</sup>, which is specified in the last column of Table (1). As underlined in Section (2.4) and Appendix D, in the latter case the approximate recursions of Section (2.2) can be applied upon re-defining the covariance matrix  $\mathbf{P}_t$  in Eq. (2.19) as  $\mathbf{P}_t = \mathbf{T}^{-1}\mathbf{A}\mathbf{S}_t$ .

The Monte Carlo study is based on 1000 replications of  $n = 4000$  observations of the state-space models described above. Each sample is divided into two sub-samples of equal size. The first sub-sample is used to estimate the model parameters by maximum likelihood, whereas the second is used to compute the mean-square-error (MSE) of the filtered (prediction and update) and smoothed estimates of the state variable  $\alpha_t$ . The results are reported in Table (2), which shows the average MSE provided by each method in the three scenarios  $q = 0.005$ ,  $q = 0.01$  and  $q = 0.05$ .

We first note that, compared to the IS method, the average loss of the score-driven methodology is negligible in the scenario  $q = 0.005$ , small (close to 2%) in the scenario  $q = 0.01$ , and substantial (larger than 8%) in the scenario  $q = 0.05$ . In the scenario  $q = 0.01$ , the average loss is close to the one found by Koopman et al. (2016), who examine the performance of score-driven models

<sup>8</sup>More precisely, in the location model,  $\mathbf{S}_t$  coincides with the inverse of the Fisher information, as in Harvey (2013). In the two stochastic volatility models, we adopt the same normalization of the Beta- $t$ -EGARCH model of Harvey (2013), in which the score is not scaled. Note that, since the Fisher information of these two models is independent from the time-varying parameter, setting  $\mathbf{S}_t = \mathbf{I}_t^{-1}$  would produce an observationally equivalent representation. Finally, in the count model, we set  $\mathbf{S}_t$  equal to the inverse of the Fisher information.



		IS	SD( $\mathbf{S}_t$ )	SD( $\mathbf{P}_t$ )	QMLE	KF	IS	SD( $\mathbf{S}_t$ )	SD( $\mathbf{P}_t$ )	QMLE	KF	IS	SD( $\mathbf{S}_t$ )	SD( $\mathbf{P}_t$ )	QMLE	KF			
		$q = 0.005$						$q = 0.01$						$q = 0.05$					
Location (Student- $t$ )	Prediction	0.0120	0.0120	0.0123	–	0.0135	0.0232	0.0235	0.0240	–	0.0270	0.1140	0.1155	0.1193	–	0.1289			
	Update	0.0066	0.0066	0.0068	–	0.0088	0.0132	0.0132	0.0134	–	0.0176	0.0646	0.0662	0.0694	–	0.0799			
	Smoother	0.0054	0.0054	0.0054	–	0.0059	0.0099	0.0102	0.0104	–	0.0115	0.0518	0.0530	0.0546	–	0.0580			
Scale (Gaussian)	Prediction	0.0736	0.0736	0.0736	0.1019	–	0.1171	0.1199	0.1189	0.1638	–	0.3247	0.3543	0.3519	0.4579	–			
	Update	0.0715	0.0715	0.0715	0.0987	–	0.1115	0.1143	0.1134	0.1592	–	0.2857	0.3165	0.3143	0.4237	–			
	Smoother	0.0537	0.0538	0.0538	0.0896	–	0.0760	0.0789	0.0770	0.1182	–	0.1823	0.2107	0.2099	0.2784	–			
Scale (Student- $t$ )	Prediction	0.0876	0.0879	0.0878	0.1428	–	0.1366	0.1392	0.1379	0.1982	–	0.3806	0.3981	0.3960	0.5030	–			
	Update	0.0859	0.0860	0.0860	0.1428	–	0.1326	0.1352	0.1332	0.1892	–	0.3442	0.3628	0.3621	0.4724	–			
	Smoother	0.0682	0.0683	0.0682	0.1382	–	0.0950	0.0961	0.0955	0.1816	–	0.2405	0.2484	0.2448	0.3516	–			
Count data (Poisson)	Prediction	0.0787	0.0789	0.0787	–	–	0.1391	0.1418	0.1408	–	–	0.4291	0.4676	0.4659	–	–			
	Update	0.0770	0.0776	0.0772	–	–	0.1311	0.1338	0.1325	–	–	0.3947	0.4337	0.4340	–	–			
	Smoother	0.0498	0.0502	0.0501	–	–	0.0759	0.0809	0.0792	–	–	0.2168	0.2729	0.2732	–	–			

**Table 2:** We report the MSE of the filtered and smoothed estimates of the four state-space models obtained through importance sampling (IS) and the score-driven (SD) algorithm of Section (2.2). In the latter case, we use both the classical normalization adopted in score-driven models (SD( $\mathbf{S}_t$ )) specified in Table (1), and the normalization in Eq. (2.21) (SD( $\mathbf{P}_t$ )). In the case of the location model, we also show the MSE of the Kalman filter (KF), whereas in the case of the two stochastic volatility models, we report the MSE of the QMLE method of Harvey et al. (1994).

assuming as data generating processes a set of state-space models having the form of Eq. (2.29), (2.30) and characterized by a similar value of  $q$ . The results of Section (2.3) and the simulation results found here provide an additional piece of information, showing that the average loss actually depends on the variance of  $\alpha_t$ , and thus on how much the underlying state-space model deviates from the particular case in which  $\alpha_t$  is non-stochastic.

It is also interesting to compare the performance of the normalization of Section (2.2) with the classical normalization adopted in score-driven models. The relative difference in MSE between the two normalization schemes is generally small. However, we note that the former tends to perform slightly better in stochastic volatility and count data models, and slightly worse in the location model. This result suggests that modeling conditional covariances as in Eq. (2.21), i.e. by letting them depend explicitly on the observations through the Hessian of the conditional density, may improve over the classical normalization scheme in models where observations depend nonlinearly on state variables. Indeed, as observed in Section (2.4), the fact that conditional covariances are independent from observations is a special property of linear Gaussian models which may not hold in general<sup>9</sup>. On the contrary, the advantage in employing the normalization of Section (2.2) disappears in the location model, which is characterized by a linear observation equation.

We finally note that the relative loss of the Kalman filter (in the location model) and QMLE (in stochastic volatility models) is significantly larger compared to the approximate score-driven algorithm. In particular, the relative performance of the Kalman filter depends on the non-normality of the simulated data, and thus on the degrees of freedom parameter and the noise-to-signal ratio, which in this analysis are set as  $\nu = 3$  and  $e^\lambda/q = 5$ , respectively. Lower values of  $\nu$  or higher values of  $e^\lambda/q$  would further increase the loss. In contrast, the loss would decrease by increasing  $\nu$  or decreasing  $e^\lambda/q$ . The QMLE, being based on the assumption of a Gaussian conditional density, exhibit a similar behavior. Note indeed that its relative loss increases in the stochastic volatility model with fat-tailed density. Not surprisingly, the computational times of the score-driven algorithm are much lower compared to the IS methodology. The ratio between the time required for estimating the static parameters and computing the filtered and smoothed estimates in the two methods ranges from 150 to 800.

Using the same Monte Carlo sample, we compute out-of-sample confidence bands around filtered and smoothed estimates by exploiting Eq. (2.42). As discussed in Section (2.6), Eq. (2.42) decomposes the conditional variance of state variables into the sum of two terms representing the contribution of filtering and parameter uncertainty. These two terms are computed by simulations,

---

<sup>9</sup>Note that, in the count data model, the Hessian is time-varying but does not depend on observations. In this particular case, the advantage of the normalization of Section (2.2) may be imputable to the particular structure of Eq. (2.21), which results from a local approximation to the true conditional second moment, thus providing a better update of time-varying parameters compared to the *ad hoc* normalization adopted in score-driven models.

		Location (Student- $t$ )		Scale (Gaussian)		Scale (Student- $t$ )		Count data (Poisson)	
		SD( $\mathbf{S}_t$ )	SD( $\mathbf{P}_t$ )	SD( $\mathbf{S}_t$ )	SD( $\mathbf{P}_t$ )	SD( $\mathbf{S}_t$ )	SD( $\mathbf{P}_t$ )	SD( $\mathbf{S}_t$ )	SD( $\mathbf{P}_t$ )
		$q = 0.005$							
Par. & Filt.	Prediction	0.9495	0.9374	0.9520	0.9533	0.9422	0.9531	0.9401	0.9471
	Update	0.9489	0.9395	0.9502	0.9504	0.9412	0.9535	0.9395	0.9461
	Smoother	0.9472	0.9493	0.9487	0.9531	0.9411	0.9544	0.9379	0.9538
Par.	Prediction	0.5320	0.5433	0.3804	0.3788	0.3667	0.3644	0.2913	0.2922
		$q = 0.01$							
Par. & Filt.	Prediction	0.9485	0.9349	0.9452	0.9482	0.9422	0.9478	0.9302	0.9366
	Update	0.9462	0.9358	0.9453	0.9480	0.9420	0.9469	0.9311	0.9353
	Smoother	0.9444	0.9401	0.9454	0.9503	0.9428	0.9482	0.9286	0.9402
Par.	Prediction	0.4915	0.4960	0.3589	0.3620	0.3583	0.3576	0.2539	0.2592
		$q = 0.05$							
Par. & Filt.	Prediction	0.9477	0.9309	0.9405	0.9425	0.9306	0.9362	0.8748	0.9021
	Update	0.9444	0.9310	0.9406	0.9426	0.9289	0.9356	0.8714	0.9017
	Smoother	0.9434	0.9363	0.9387	0.9420	0.9247	0.9306	0.8708	0.9040
Par.	Prediction	0.2002	0.2128	0.3210	0.3120	0.2998	0.2912	0.1233	0.1370

**Table 3:** This table shows the average coverage rates of the out-of-sample confidence bands constructed around filtered and smoothed estimates at confidence level 95% for  $q = 0.005, 0.01, 0.05$ . For each model, we report the results obtained with the classical normalization adopted in score-driven models (SD( $\mathbf{S}_t$ )) specified in Table (1), and the normalization in Eq. (2.21) (SD( $\mathbf{P}_t$ )). We also report the average coverage rates obtained using the method of Blasques et al. (2016), which only accounts for parameter uncertainty.

sampling the static parameters from a normal distribution with mean equal to the maximum likelihood estimates and variance given by the negative inverse Hessian matrix of the log-likelihood. The confidence bands are then given by the quantiles of a normal distribution with mean equal to the filtered (smoothed) estimates, and variance given by the sum of the two terms in Eq. (2.42).

The confidence bands are computed at confidence level  $\alpha = 0.95$ . As a benchmark, we consider the simulation-based method of Blasques et al. (2016). This method samples the static parameters from the asymptotic distribution of the maximum likelihood estimates and, for any sampled parameter, builds the path of one-step-ahead predictions. The confidence bands computed from the distribution of the sampled paths account for parameter uncertainty but ignore filtering uncertainty.

Table (3) shows the average coverage rates of the confidence bands constructed using the two approaches. As in the previous analysis, to implement the score-driven recursions we use both the normalization of Section (2.2) and the classical normalization adopted in score-driven models. For

$q = 0.005$ , the algorithm based on score-driven recursions provides a close match to the nominal confidence level. As  $q$  increases, the confidence bands constructed with this approach tend to become narrow, with coverage rates which are below the nominal confidence level. This effect is particularly evident in the count data model, whose coverage rates are substantially lower than 0.95 for  $q = 0.05$ , whereas it is less pronounced in the other models. We thus find the same effect observed in the previous analysis, imputable to the deterioration of the approximation with increasing  $q$ . Even the behavior of the two normalization schemes is similar to that observed in the previous analysis. They generally provide close results, with the normalization based on Eq. (2.21) slightly out-performing the classical normalization  $\mathbf{S}_t$  in the three nonlinear models. It is important to note that neglecting filtering uncertainty severely underestimates the total uncertainty, as can be seen from the small coverage rates of the method of Blasques et al. (2016). The fact that the latter provides very narrow confidence bands is due to the very different dynamics followed by the underlying state variable  $\alpha_t$ , given by Eq. (3.1), and the simulated one-step-ahead predictions used to construct confidence bands. We thus conclude that accounting for filtering uncertainty is essential to accurately compute confidence bands when using score-driven models to approximate the behavior of nonlinear non-Gaussian state-space models.

## 4 Empirical applications

In this section we provide empirical evidences that employing observation-driven models as approximate filters offers a more complete and accurate description of the dynamics of time-varying parameters. Volatility modeling represents an ideal empirical framework for this purpose, because it allows us to assess the performance of the methodology by comparing the approximate filtered and smoothed estimates of stochastic volatility models with the realized volatility computed from high-frequency data. The latter provides a precise proxy of the unobserved volatility process that can be used as a benchmark in loss measures; see Andersen and Bollerslev (1997), Andersen et al. (2003), Barndorff-Nielsen and Shephard (2004). However, we emphasize that the methodology remains formally unchanged in empirical problems characterized by different time-varying parameters and different conditional distributions.

Let us consider the following two-component stochastic volatility model:

$$y_t = e^{\frac{\theta_t}{2}} \epsilon_t \tag{4.1}$$

$$\theta_t = \omega + \mathbf{Z}\alpha_t \tag{4.2}$$

$$\alpha_{t+1} = \mathbf{T}\alpha_t + \eta_t, \quad \eta_t \sim \mathbf{N}(\mathbf{0}, \mathbf{Q}) \tag{4.3}$$

where  $\epsilon_t \sim t_\nu$ ,  $\mathbf{Z} = (1, 1)$ ,  $\mathbf{T} = \text{diag}(\phi_1, \phi_2)$  and  $\mathbf{Q} \in \mathbb{R}^{2 \times 2}$ . Stochastic volatility models with two volatility components have been advocated for instance by Engle and Lee (1999), Alizadeh

et al. (2002), Andersen et al. (2006), Harvey and Lange (2018), and are known to display long memory behaviour. The two volatility components can be interpreted as representing a slow factor responsible for the long-term dynamics of volatility, and a fast factor responsible for the after-shocks following large volatility movements; see also Harvey (2013) for a discussion.

We work with 1-minute transaction data of ExxonMobil (XOM) over the period from 01-12-1999 to 27-09-2013, which includes 3478 business days. For each day  $t$ , we construct (i) the daily return  $y_t$  computed as the difference between the closing and the opening log-prices, and (ii) the realized variance  $RV_t$  obtained as the sum of 5-minutes squared returns.  $RV_t$  is a consistent estimator of the (integrated) daily variance of the continuous-time process describing asset returns. Thus, for the purpose of computing the mean-square errors and assessing the average coverage of the confidence bands, we can use  $\log RV_t$  as if it was the true latent log-variance  $\theta_t$ .

To run the recursions of Section (2.2), we set  $p(y_t|Y_{t-1}) = p(y_t|\theta_t)|_{\kappa_t}$ , namely:

$$\begin{aligned} \log p(y_t|Y_{t-1}) = & \log \Gamma\left(\frac{\nu+1}{2}\right) - \log \Gamma\left(\frac{\nu}{2}\right) - \frac{1}{2} \log \pi - \frac{1}{2} \log(\nu-2) \\ & - \frac{\kappa_t}{2} - \frac{\nu+1}{2} \log \left[ 1 + \frac{y_t^2}{(\nu-2)e^{\kappa_t}} \right] \end{aligned} \quad (4.4)$$

where  $\kappa_t = \omega + \mathbf{Z}\mathbf{a}_t$  and  $\mathbf{a}_t$  is computed iteratively through Eq. (2.19), (2.21). The normalization of the score is set as in Eq. (2.21). Contrary to the classical normalization adopted in score-driven models, such choice allows us to uniquely identify the conditional covariance  $\mathbf{P}_t$  and the smoother, as discussed in appendix E.

The parameters  $\nu$ ,  $\omega$ ,  $\mathbf{T}$ ,  $\mathbf{Q}$  are estimated in the first sub-sample of  $n = 2000$  business days. The out-of-sample filtered and smoothed estimates are then computed in the remaining sub-sample of 1478 days, from 14-11-2007 to 27-09-2013. In the following, we report the estimates of the model parameters obtained by optimizing the sum of the conditional log-likelihoods in Eq. (4.4):

$$\begin{aligned} \tilde{\omega} = 0.0101, \quad \tilde{\phi}_1 = 0.9992, \quad \tilde{\phi}_2 = 0.9088, \quad \tilde{\nu} = 9.7201 \\ \tilde{\mathbf{Q}}_{11} = 0.0037, \quad \tilde{\mathbf{Q}}_{22} = 0.0165, \quad \tilde{\mathbf{Q}}_{12} = 0.0073 \end{aligned}$$

As commonly found in two-component models, the slow factor has large persistence ( $\tilde{\phi}_1 \approx 1$ ) and lower variance ( $\tilde{\mathbf{Q}}_{11} \ll \tilde{\mathbf{Q}}_{22}$ ). Figures (1) and (2) show out-of-sample filtered and smoothed estimates of the two volatility factors, whereas Figure (3) shows the out-of-sample log-variance obtained by summing the two factors and adding the intercept  $\tilde{\omega}$ .

To assess the extent to which the filtered and smoothed variances are accurate estimates of the latent variance process, we compute the out-of-sample mean-square error (MSE) and the quasi-likelihood (Qlike) measure described by Patton and Sheppard (2009):

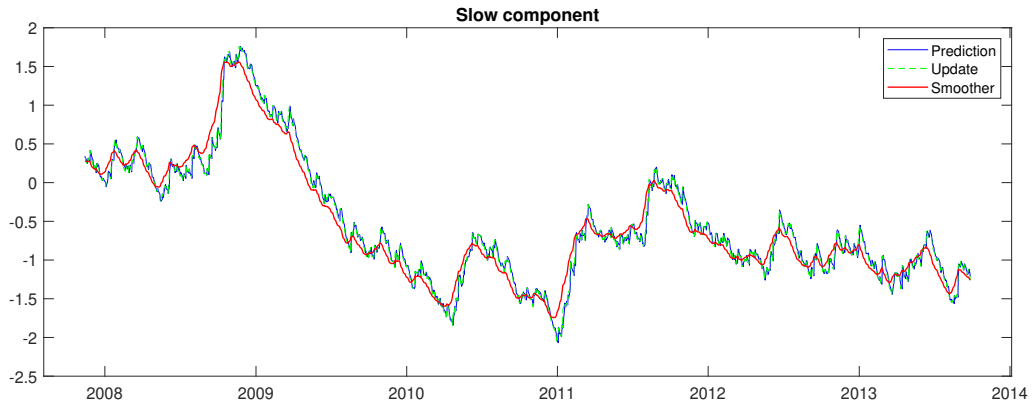


**Figure 1:** We show the out-of-sample filtered and smoothed estimates of the slow volatility component  $\alpha_t^{(1)}$  of XOM.

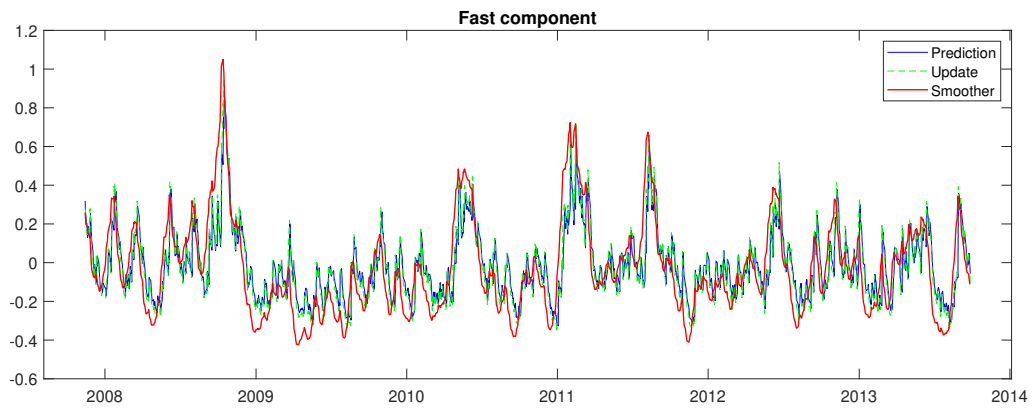


**Figure 2:** We show the out-of-sample filtered and smoothed estimates of the fast volatility component  $\alpha_t^{(2)}$  of XOM.

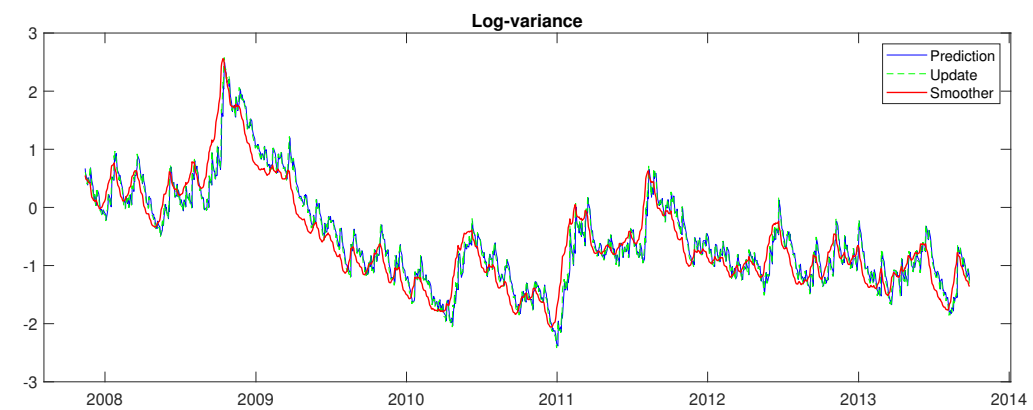


**Figure 3:** We show the out-of-sample filtered and smoothed estimates of the log-variance  $\theta_t = \omega + \mathbf{Z}\alpha_t$  of XOM.

$$\begin{aligned}
\text{MSE}^{(p)} &= \frac{1}{1478} \sum_{t=2001}^{3478} (\log RV_t - \kappa_t)^2, & \text{Qlike}^{(p)} &= \frac{1}{1478} \sum_{t=2001}^{3478} \left( \frac{RV_t}{e^{\kappa_t}} - \log \frac{RV_t}{e^{\kappa_t}} - 1 \right) \\
\text{MSE}^{(u)} &= \frac{1}{1478} \sum_{t=2001}^{3478} (\log RV_t - \kappa_{t|t})^2, & \text{Qlike}^{(u)} &= \frac{1}{1478} \sum_{t=2001}^{3478} \left( \frac{RV_t}{e^{\kappa_{t|t}}} - \log \frac{RV_t}{e^{\kappa_{t|t}}} - 1 \right) \\
\text{MSE}^{(s)} &= \frac{1}{1478} \sum_{t=2001}^{3478} (\log RV_t - \hat{\kappa}_t)^2, & \text{Qlike}^{(s)} &= \frac{1}{1478} \sum_{t=2001}^{3478} \left( \frac{RV_t}{e^{\hat{\kappa}_t}} - \log \frac{RV_t}{e^{\hat{\kappa}_t}} - 1 \right)
\end{aligned}$$

where  $\kappa_t$ ,  $\kappa_{t|t}$  and  $\hat{\kappa}_t$  denote the predictive filter, the update filter and the smoother, respectively. We find the following numerical values for the loss measures:

$$\begin{aligned}
\text{MSE}^{(p)} &= 0.3396, & \text{MSE}^{(u)} &= 0.3021, & \text{MSE}^{(s)} &= 0.2640^* \\
\text{Qlike}^{(p)} &= 0.2683, & \text{Qlike}^{(u)} &= 0.2179, & \text{Qlike}^{(s)} &= 0.1871^*
\end{aligned}$$

The star symbol denotes that the corresponding loss measure is significantly smaller than others, as resulting from the Model Confidence Set (MCS) test of Hansen et al. (2011) at 90% confidence level. In particular, observe that  $\text{MSE}^{(s)}$  is significantly smaller than both  $\text{MSE}^{(p)}$  and  $\text{MSE}^{(u)}$ , and the same happens for the Qlike measure. This result suggests that volatility is not completely revealed by past observations, as a correctly specified observation-driven model would suggest, and that exploiting the information of contemporaneous and future returns helps to improve the estimation of volatility.

As highlighted above, the covariance matrix  $\mathbf{P}_t$  and the smoother would not be uniquely identifiable if normalizing the score using the classical normalization matrix adopted in score-driven models, e.g. if setting  $\mathbf{S}_t = \mathbf{I}$ . However, as evidenced in Appendix E, the predictive and update filter would still be uniquely determined. In line with the results of the Monte-Carlo study in Section (3), we find that the performance of these two filters does not change substantially under a different normalization. For instance, if the scaling matrix is set equal to the identity matrix, we obtain the following loss measures for the predictive and update filters:

$$\begin{aligned}
\text{MSE}^{(p)} &= 0.3403, & \text{MSE}^{(u)} &= 0.3036 \\
\text{Qlike}^{(p)} &= 0.2655, & \text{Qlike}^{(u)} &= 0.2119
\end{aligned}$$

which are very similar to the analogous loss measures provided by the normalization in Eq. (2.21).

In light of such results, we expect that filtering uncertainty plays a role when building confidence bands. To verify that this is the case, we construct the out-of-sample confidence bands as described in Section (2.6) and in the second part of Section (3). Table (4) shows the average coverage rates of the confidence bands at different nominal confidence levels, together with the coverage rates of the method of Blasques et al. (2016). As in the Monte Carlo analysis, we find that neglecting filtering uncertainty leads to underestimate the total uncertainty around the filtered and smoothed estimates. In order to describe better this phenomenon, we plot in Fig. (4) the out-of-sample

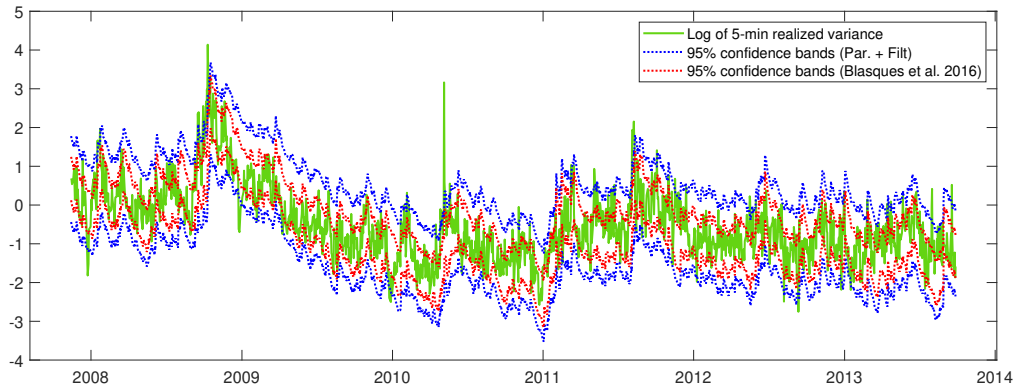


**Figure 4:** We show: the logarithm of the 5-minute realized variance of XOM in the period from 14 Nov. 2007 to 27 Sep. 2013 (green); the out-of-sample 95% confidence bands of the predicted filter computed by accounting for parameter and filtering uncertainty (blue); the out-of-sample 95% confidence bands computed with the simulation-based method of Blasques et al. (2016) accounting for parameter uncertainty only (red).

confidence bands obtained with the two methods, and the time-series of logarithmic daily realized variance. We clearly see that ignoring filtering uncertainty leads to narrow confidence bands and to a number of exceedances larger than what expected based on the choice of the nominal confidence level.

		$\alpha = 0.90$	$\alpha = 0.95$	$\alpha = 0.99$
Par. & Filt.	Prediction	0.9039	0.9513	0.9817
	Update	0.9114	0.9520	0.9851
	Smoother	0.8857	0.9381	0.9811
Par.	Prediction	0.6461	0.6922	0.7930

**Table 4:** For the asset XOM, we report the average coverage rates of the out-of-sample confidence bands constructed around filtered and smoothed estimates at confidence levels  $\alpha = 0.90, 0.95, 0.99$ . For the predictive filter, we also report the average coverage rate obtained through the method of Blasques et al. (2016), which only accounts for parameter uncertainty.

So far, we have been focusing on univariate time-series. It is also interesting to verify whether the recovered results hold for a multivariate time-series of stock returns. To this end, we consider a dataset of 1-minute transaction data of 4166 Russel 3000 constituents covering the period from 18-11-1999 to 27-09-2013. In order to avoid discontinuities due to changes in index composition, we concentrate on the sub-sample comprising the last 2000 business days. Assets having less than 10 trades per day are excluded in order to avoid poor and/or ill-conditioned realized covariance estimates. As a final outcome, we end up with 1682 assets.

Since we deal with multivariate time-series, we need a dynamic covariance model for vectors of log-returns. In this application, we consider the  $t$ -GAS model of Creal et al. (2011), which is



	Portfolio 1	Portfolio 2	Portfolio 3	Portfolio 4
	MSE $\times 10^5$			
Prediction	0.7061	0.3705	0.2146	0.3255
Update	0.6950*	0.3634*	0.2099	0.3170*
Smoother	0.6709*	0.3565*	0.1998*	0.3046*
	Qlike			
Prediction	-134.7951	-128.6277	-140.1625	-137.9562
Update	-135.1702	-129.0375	-140.5694	-138.2863
Smoother	-135.7584*	-129.3180*	-141.2055*	-138.8856*

**Table 5:** MSE and Qlike of filtered and smoothed estimates of the  $t$ -GAS model for the four randomly selected portfolios of  $p = 20$  assets. Stars denote the fact that the corresponding estimate is included in the MCS at 90% confidence level.

based on a multivariate Student- $t$  conditional density. To guarantee positive-definite estimates, we implement the parameterization based on hyperspherical coordinates, as detailed by Creal et al. (2011). Since the matrix  $\mathbf{A}$  multiplying the score is uniquely identifiable, we set the score normalization equal to the inverse of the Fisher information matrix. The number of time-varying parameters grows as  $p^2$ , where  $p$  is the number of assets. As such, we can test the performance of our approximate filtering methodology in a highly multivariate framework where the use of exact simulation-based methods is computationally problematic or even unfeasible.

Among the universe of  $N = 1682$  assets, we randomly choose four portfolios of  $p = 20$  assets. The loss measures used in this analysis are the MSE, computed as the Frobenius norm between matrices, and the multivariate Qlike; see e.g. Patton and Sheppard (2009). As a realized covariance estimator, we employ the estimator of Barndorff-Nielsen and Shephard (2004), computed as the dot product of 5-minute log-returns. For each portfolio, the  $t$ -GAS is estimated on the first sub-sample of 1000 business days. We then compute, in the remaining sub-sample, the predictive filter, the update filter and the smoother. The statistical significance of loss differences is tested through the MCS at 90% confidence level.

Table (5) shows the results of the analysis. Even in this multivariate application, we find that the covariance estimates constructed through the predictive filter feature larger MSE and Qlike, and are always excluded from the MCS. The covariance estimates built through the update filter and the smoother are both included in the MCS when considering the MSE as a loss measure. If the Qlike is instead considered, only smoothed estimates are included. Such results are in line with those found in the univariate application, and confirm the relevance of employing observation-driven models as approximate filters.

## 5 Conclusions

Correctly specified observation-driven models are purely predictive, meaning that past observations include all the relevant information concerning the dynamics of time-varying parameters. As such, there is no room for smoothing, and the only form of uncertainty comes from replacing the true static parameters with their maximum-likelihood estimates.

In this paper, we adopt a different view and assume that observation-driven models are approximate filters. This means that the process generating the data is not the observation-driven model itself, but rather a nonlinear non-Gaussian state-space model. In this framework, time-varying parameters are not completely revealed by past observations, and thus one needs a methodology for smoothing and assessing filtering uncertainty.

Starting from a general representation of the Kalman filter and smoothing recursions in terms of the score of the conditional density, we recover an approximate methodology for estimating the first two conditional moments of the underlying state variables. This also allows us to compute, in addition to classical one-step-ahead predictions, the update filter, the smoother, and to build in-sample and out-of-sample confidence bands accounting for both parameter and filtering uncertainty.

We prove that, under the assumption that data is generated by a nonlinear non-Gaussian state-space model, the proposed filtering algorithm results from a local expansion of the true filtering density around the particular case in which state variables are non-stochastic. Such result allows us to formally characterize the approximation error made in replacing the optimal filter with the approximate score-driven filter.

In the simulation study, we find a small loss when comparing our approximate method with importance sampling in a wide range of scenarios. However, it is worth highlighting that the exact simulation-based methods are much more expensive from a computational point of view, requiring Monte Carlo integration and the choice of an importance density. Filtering uncertainty plays a key role when computing confidence bands in score-driven models. We show in simulations that neglecting filtering uncertainty leads to narrow confidence bands and to a number of exceedances significantly larger than what expected from the choice of the nominal confidence level.

These results have relevant consequences when applying observation-driven models to real data. If the latter are better described by a nonlinear non-Gaussian model, the use of correctly specified observation-driven models may be too restrictive, as they would not allow to exploit the information of contemporaneous and future observations. Furthermore, it leads to narrow confidence bands, which may have deep policy and institutional implications. These findings are evidenced on empirical data using both univariate and multivariate stochastic volatility models, which are readily implementable in our methodology.

## References

- Alizadeh, S., Brandt, M.W., Diebold, F.X., 2002. Range-based estimation of stochastic volatility models. *The Journal of Finance* 57, 1047–1091.
- Andersen, T., Bollerslev, T., 1997. Intraday periodicity and volatility persistence in financial markets. *Journal of Empirical Finance* 4, 115–158.
- Andersen, T.G., Bollerslev, T., Christoffersen, P.F., Diebold, F.X., 2006. Volatility and Correlation Forecasting. Elsevier. volume 1 of *Handbook of Economic Forecasting*. chapter 15. pp. 777–878.
- Andersen, T.G., Bollerslev, T., Diebold, F.X., Labys, P., 2003. Modeling and forecasting realized volatility. *Econometrica* 71, 579–625.
- Anderson, B., Moore, J., 1979. *Optimal Filtering*. Prentice-Hall, Englewood Cliffs, NJ.
- Babii, A., Chen, X., Ghysels, E., 2019. Commercial and residential mortgage defaults: Spatial dependence with frailty. *Journal of Econometrics* 212, 47 – 77.
- Barndorff-Nielsen, O.E., Shephard, N., 2004. Econometric analysis of realized covariation: High frequency based covariance, regression, and correlation in financial economics. *Econometrica* 72, 885–925.
- Blasques, F., Koopman, S.J., Lasak, K., Lucas, A., 2016. In-sample confidence bands and out-of-sample forecast bands for time-varying parameters in observation-driven models. *International Journal of Forecasting* 32, 875 – 887.
- Blasques, F., Koopman, S.J., Lucas, A., 2015. Information-theoretic optimality of observation-driven time series models for continuous responses. *Biometrika* 102, 325.
- Bollerslev, T., 1986. Generalized autoregressive conditional heteroskedasticity. *Journal of Econometrics* 31, 307–327.
- Buccheri, G., Corsi, F., Flandoli, F., Livieri, G., 2020. The continuous-time limit of score-driven volatility models. *Journal of Econometrics* .
- Caivano, M., Harvey, A., Luati, A., 2016. Robust time series models with trend and seasonal components. *SERIEs* 7, 99–120.
- Cox, D., 1981. Statistical analysis of time series: Some recent developments [with discussion and reply]. *Scandinavian Journal of Statistics* 8, 93–115.
- Creal, D., Koopman, S.J., Lucas, A., 2011. A dynamic multivariate heavy-tailed model for time-varying volatilities and correlations. *Journal of Business & Economic Statistics* 29, 552–563.

- Creal, D., Koopman, S.J., Lucas, A., 2013. Generalized autoregressive score models with applications. *Journal of Applied Econometrics* 28, 777–795.
- Durbin, J., Koopman, S., 2012. *Time Series Analysis by State Space Methods: Second Edition*. Oxford Statistical Science Series, OUP Oxford.
- Durbin, J., Koopman, S.J., 1997. Monte Carlo maximum likelihood estimation for non-Gaussian state space models. *Biometrika* 84, 669–684.
- Engle, R., 1982. Autoregressive conditional heteroscedasticity with estimates of the variance of United Kingdom inflation. *Econometrica* 50, 987–1007.
- Engle, R.F., Lee, G.G.J., 1999. A long-run and short-run component model of stock return volatility. Oxford University Press. *Cointegration, Causality and Forecasting: A Festschrift in Honour of Clive W. J. Granger*.
- Fleming, W.H., 1971. Stochastic control for small noise intensities. *SIAM Journal on Control* 9, 473–517.
- Hamilton, J.D., 1986. A standard error for the estimated state vector of a state-space model. *Journal of Econometrics* 33, 387 – 397.
- Hansen, P.R., Lunde, A., Nason, J.M., 2011. The model confidence set. *Econometrica* 79, 453–497.
- Harvey, A., 1991. *Forecasting, Structural Time Series Models and the Kalman Filter*. Cambridge University Press.
- Harvey, A., Lange, R.J., 2018. Modeling the interactions between volatility and returns using egarch-m. *Journal of Time Series Analysis* 39, 909–919.
- Harvey, A., Luati, A., 2014. Filtering with heavy tails. *Journal of the American Statistical Association* 109, 1112–1122.
- Harvey, A., Ruiz, E., Shephard, N., 1994. Multivariate stochastic variance models. *The Review of Economic Studies* 61, 247–264.
- Harvey, A.C., 2013. *Dynamic Models for Volatility and Heavy Tails: With Applications to Financial and Economic Time Series*. Cambridge University Press. *Econometric Society Monographs*.
- Komunjer, I., Sizova, N., 2018. A Perturbation Approach to Nonlinear Filtering: The Case of Stochastic Volatility. Technical Report. Available at SSRN: <https://ssrn.com/abstract=3281037>.
- Koopman, S.J., Lucas, A., Scharth, M., 2015. Numerically accelerated importance sampling for nonlinear non-Gaussian state-space models. *Journal of Business & Economic Statistics* 33, 114–127.

- Koopman, S.J., Lucas, A., Scharth, M., 2016. Predicting time-varying parameters with parameter-driven and observation-driven models. *The Review of Economics and Statistics* 98, 97–110.
- Linton, O., Wu, J., 2020. A Coupled Component DCS-EGARCH Model for Intraday and Overnight Volatility. *Journal of Econometrics* 217, 176–201.
- Lucas, A., Schaumburg, J., Schwaab, B., 2019. Bank business models at zero interest rates. *Journal of Business & Economic Statistics* 37, 542–555.
- Masreliez, C.J., 1975. Approximate non-Gaussian filtering with linear state and observation relations. *IEEE Transactions on Automatic Control* AC-20, 777–795.
- Nelson, D.B., 1992. Filtering and forecasting with misspecified ARCH models I: Getting the right variance with the wrong model. *Journal of Econometrics* 52, 61 – 90.
- Nelson, D.B., 1996. Asymptotically optimal smoothing with ARCH models. *Econometrica* 64, 561–573.
- Nelson, D.B., Foster, D.P., 1994. Asymptotic filtering theory for univariate ARCH models. *Econometrica* 62, 1–41.
- Nelson, D.B., Foster, D.P., 1995. Filtering and forecasting with misspecified ARCH models II: Making the right forecast with the wrong model. *Journal of Econometrics* 67, 303 – 335.
- Oh, D.H., Patton, A.J., 2017. Time-varying systemic risk: Evidence from a dynamic copula model of cds spreads. *Journal of Business & Economic Statistics* 0, 1–15.
- Pascual, L., Romo, J., Ruiz, E., 2006. Bootstrap prediction for returns and volatilities in GARCH models. *Computational Statistics & Data Analysis* 50, 2293 – 2312.
- Patton, A.J., Sheppard, K., 2009. *Evaluating Volatility and Correlation Forecasts*. Springer Berlin Heidelberg, Berlin, Heidelberg. pp. 801–838.
- Shephard, N., Pitt, M.K., 1997. Likelihood analysis of non-Gaussian measurement time series. *Biometrika* 84, 653–667.
- Sorenson, H., Alspach, D., 1971. Recursive bayesian estimation using gaussian sums. *Automatica* 7, 465 – 479.
- Sorenson, H.W., Stubberud, A.R., 1968. Non-linear filtering by approximation of the a posteriori density. *International Journal of Control* 8, 33–51.

# Appendix

Before showing the proofs of the main results, we prove the following lemma:

**Lemma 1.** *Assume that for all  $b \in \mathbb{R}$ , there exists  $\bar{\delta} > 0$  such that  $p(\alpha_t|\alpha_{t-1}) < \frac{1}{|\alpha_t - b|^{k+\beta}}$ ,  $k \in \mathbb{N}$ ,  $\beta > 0$ , for all  $\alpha_t$  such that  $|\alpha_t - b| > \bar{\delta}$ . Then also  $p(\alpha_t|Y_{t-1}) < \frac{1}{|\alpha_t - b|^{k+\beta}}$  for all  $\alpha_t$  such that  $|\alpha_t - b| > \bar{\delta}$ .*

*Proof.* Observe that we can write:

$$\begin{aligned} p(\alpha_t|Y_{t-1}) &= \frac{p(\alpha_t, Y_{t-1})}{p(Y_{t-1})} = \frac{1}{p(Y_{t-1})} \int_{\mathbb{R}^{t-1}} p(\alpha_1, \dots, \alpha_t, y_1, \dots, y_{t-1}) d\alpha_1 \dots d\alpha_{t-1} \\ &= \frac{1}{p(Y_{t-1})} \int_{\mathbb{R}^{t-1}} \left( \prod_{j=1}^{t-1} p(y_j|\alpha_j) p(\alpha_j|\alpha_{j-1}) \right) p(\alpha_t|\alpha_{t-1}) d\alpha_1 \dots d\alpha_{t-1} \end{aligned}$$

For  $\alpha_t$  such that  $|\alpha_t - b| > \bar{\delta}$  we have:

$$p(\alpha_t|Y_{t-1}) < \frac{1}{|\alpha_t - b|^{k+\beta}} \frac{1}{p(Y_{t-1})} \int_{\mathbb{R}^{t-1}} \prod_{j=1}^{t-1} p(y_j|\alpha_j) p(\alpha_j|\alpha_{j-1}) d\alpha_1 \dots d\alpha_{t-1} = \frac{1}{|\alpha_t - b|^{k+\beta}}$$

because  $\int_{\mathbb{R}^{t-1}} \prod_{j=1}^{t-1} p(y_j|\alpha_j) p(\alpha_j|\alpha_{j-1}) d\alpha_1 \dots d\alpha_{t-1} = p(Y_{t-1})$ . □

## A Proof of Proposition 1

We can write the conditional density  $p(y_t|Y_{t-1})$  as:

$$p(y_t|Y_{t-1}) = \int_{-\infty}^{+\infty} p(y_t|\alpha_t) p(\alpha_t|Y_{t-1}) d\alpha_t \quad (\text{A.1})$$

Let  $\delta > \bar{\delta}$ , where  $\bar{\delta}$  is defined in Assumption 2. Expanding  $p(y_t|\alpha_t)$  at first order in a neighborhood of center  $a_t$  and radius  $\delta$ , we obtain:

$$p(y_t|\alpha_t) = p(y_t|\alpha_t)|_{a_t} + \frac{\partial p(y_t|\alpha_t)}{\partial \alpha_t} \Big|_{a_t} (\alpha_t - a_t) + g(\alpha_t) \quad (\text{A.2})$$

where  $g(\alpha_t)$  is a function such that  $|g(\alpha_t)| < M(\delta)(\alpha_t - a_t)^2$  for each  $\alpha_t$  belonging to the neighborhood. Thanks to Assumption 1, the constant  $M(\delta)$  is given by  $M(\delta) = \frac{1}{2} \sup_{|\alpha_t - a_t| < \delta} \left| \frac{\partial^2 p(y_t|\alpha_t)}{\partial \alpha_t^2} \right|$ .

We can thus write the integral in Eq. (A.1) as:

$$\begin{aligned} p(y_t|Y_{t-1}) &= \int_{-\infty}^{+\infty} \left[ p(y_t|\alpha_t)|_{a_t} + \frac{\partial p(y_t|\alpha_t)}{\partial \alpha_t} \Big|_{a_t} (\alpha_t - a_t) + g(\alpha_t) \right] p(\alpha_t|Y_{t-1}) d\alpha_t \\ &= p(y_t|\alpha_t)|_{a_t} + \int_{-\infty}^{+\infty} g(\alpha_t) p(\alpha_t|Y_{t-1}) d\alpha_t \end{aligned}$$

Let us decompose the integral over  $g(\alpha_t)$  as:

$$\begin{aligned} \int_{-\infty}^{+\infty} g(\alpha_t) p(\alpha_t|Y_{t-1}) d\alpha_t &= \int_{-\infty}^{a_t - \delta} g(\alpha_t) p(\alpha_t|Y_{t-1}) d\alpha_t \\ &\quad + \int_{a_t - \delta}^{a_t + \delta} g(\alpha_t) p(\alpha_t|Y_{t-1}) d\alpha_t + \int_{a_t + \delta}^{+\infty} g(\alpha_t) p(\alpha_t|Y_{t-1}) d\alpha_t \end{aligned}$$

Observe that the second integral can be bounded as follows:

$$\begin{aligned}
\left| \int_{a_t-\delta}^{a_t+\delta} g(\alpha_t) p(\alpha_t | Y_{t-1}) d\alpha_t \right| &\leq \int_{a_t-\delta}^{a_t+\delta} |g(\alpha_t)| p(\alpha_t | Y_{t-1}) d\alpha_t \\
&\leq \int_{a_t-\delta}^{a_t+\delta} M(\delta) (\alpha_t - a_t)^2 p(\alpha_t | Y_{t-1}) d\alpha_t \\
&\leq M(\delta) p_t
\end{aligned}$$

To bound the first and third integrals, we use the condition in Assumption 2 and Lemma 1. Let us focus on the third integral:

$$\begin{aligned}
\left| \int_{a_t+\delta}^{+\infty} g(\alpha_t) p(\alpha_t | Y_{t-1}) d\alpha_t \right| &\leq \int_{a_t+\delta}^{+\infty} |g(\alpha_t)| p(\alpha_t | Y_{t-1}) d\alpha_t \\
&= \int_{a_t+\delta}^{+\infty} \left| p(y_t | \alpha_t) - p(y_t | \alpha_t) \Big|_{a_t} - \frac{\partial p(y_t | \alpha_t)}{\partial \alpha_t} \Big|_{a_t} (\alpha_t - a_t) \right| p(\alpha_t | Y_{t-1}) d\alpha_t \\
&\leq \int_{a_t+\delta}^{+\infty} \frac{\sup_{\alpha_t > a_t+\delta} p(y_t | \alpha_t) + p(y_t | \alpha_t) \Big|_{a_t}}{(\alpha_t - a_t)^{3+\beta}} d\alpha_t \\
&\quad + \int_{a_t+\delta}^{+\infty} \left| \frac{\partial p(y_t | \alpha_t)}{\partial \alpha_t} \Big|_{a_t} \right| \frac{1}{(\alpha_t - a_t)^{2+\beta}} d\alpha_t
\end{aligned}$$

where the second inequality is due to the boundedness of  $p(y_t | \alpha_t)$  and to the restriction that  $\delta > \bar{\delta}$ .

Computing the two integrals we get:

$$\begin{aligned}
\left| \int_{a_t+\delta}^{+\infty} g(\alpha_t) p(\alpha_t | Y_{t-1}) d\alpha_t \right| &\leq \frac{1}{2+\beta} \frac{\sup_{\alpha_t > a_t+\delta} p(y_t | \alpha_t) + p(y_t | \alpha_t) \Big|_{a_t}}{\delta^{2+\beta}} \\
&\quad + \frac{1}{1+\beta} \left| \frac{\partial p(y_t | \alpha_t)}{\partial \alpha_t} \Big|_{a_t} \right| \frac{1}{\delta^{1+\beta}}
\end{aligned}$$

Similarly, the first integral can be bounded as:

$$\begin{aligned}
\left| \int_{-\infty}^{a_t+\delta} g(\alpha_t) p(\alpha_t | Y_{t-1}) d\alpha_t \right| &\leq \frac{1}{2+\beta} \frac{\sup_{\alpha_t < a_t-\delta} p(y_t | \alpha_t) + p(y_t | \alpha_t) \Big|_{a_t}}{\delta^{2+\beta}} \\
&\quad + \frac{1}{1+\beta} \left| \frac{\partial p(y_t | \alpha_t)}{\partial \alpha_t} \Big|_{a_t} \right| \frac{1}{\delta^{1+\beta}}
\end{aligned}$$

We choose  $\tilde{\delta}$  such that  $\tilde{\delta} > \max(\bar{\delta}, \delta^*)$ , where  $\delta^*$  denotes the lowest  $\delta$  for which the following inequality holds:

$$\frac{1}{2+\beta} \frac{\sup_{\alpha_t < a_t-\delta} p(y_t | \alpha_t) + \sup_{\alpha_t > a_t+\delta} p(y_t | \alpha_t) + 2p(y_t | \alpha_t) \Big|_{a_t}}{\delta^{2+\beta}} + \frac{2}{1+\beta} \left| \frac{\partial p(y_t | \alpha_t)}{\partial \alpha_t} \Big|_{a_t} \right| \frac{1}{\delta^{1+\beta}} < \gamma$$

Setting  $\xi_t = \int_{-\infty}^{+\infty} g(\alpha_t) p(\alpha_t | Y_{t-1}) d\alpha_t$ , we can write  $p(y_t | Y_{t-1})$  as:

$$p(y_t | Y_{t-1}) = p(y_t | \alpha_t) \Big|_{a_t} + \xi_t$$

with  $|\xi_t| \leq \frac{1}{2} \sup_{|\alpha_t - a_t| < \tilde{\delta}} \left| \frac{\partial^2 p(y_t | \alpha_t)}{\partial \alpha_t^2} \right| p_t + \gamma$ .

□

## B Proof of Theorem 1

We first observe that, thanks to the Bayes rule, we can write:

$$p(\alpha_t|Y_t) = \frac{p(y_t|\alpha_t)p(\alpha_t|Y_{t-1})}{p(y_t|Y_{t-1})}$$

Thus, the first conditional moment  $a_{t|t}$  of  $p(\alpha_t|Y_t)$  can be computed as:

$$a_{t|t} = \int_{-\infty}^{+\infty} \alpha_t p(\alpha_t|Y_t) d\alpha_t = \int_{-\infty}^{+\infty} \alpha_t \frac{p(y_t|\alpha_t)p(\alpha_t|Y_{t-1})}{p(y_t|Y_{t-1})} d\alpha_t$$

As in Appendix A, let us consider the first order expansion of  $p(y_t|\alpha_t)$  in Eq. (A.2):

$$p(y_t|\alpha_t) = p(y_t|\alpha_t)|_{a_t} + \left. \frac{\partial p(y_t|\alpha_t)}{\partial \alpha_t} \right|_{a_t} (\alpha_t - a_t) + g(\alpha_t)$$

where  $|g(\alpha_t)| < M(\delta)(\alpha_t - a_t)^2$  for each  $\alpha_t$  belonging to a neighborhood of center  $a_t$  and radius  $\delta$ . The constant  $M(\delta)$  is given by  $M(\delta) = \frac{1}{2} \sup_{|\alpha_t - a_t| < \delta} \left| \frac{\partial^2 p(y_t|\alpha_t)}{\partial \alpha_t^2} \right|$  thanks to Assumption 1. We set  $\delta > \bar{\delta}$ , where  $\bar{\delta}$  is defined in Assumption 3. We can thus write:

$$a_{t|t} = \frac{p(y_t|\alpha_t)|_{a_t}}{p(y_t|Y_{t-1})} \int_{-\infty}^{+\infty} \alpha_t \left[ 1 + \nabla_t(\alpha_t - a_t) + \frac{g(\alpha_t)}{p(y_t|\alpha_t)|_{a_t}} \right] p(\alpha_t|Y_{t-1}) d\alpha_t$$

Let us compute the integral of the first two terms:

$$\begin{aligned} & \int_{-\infty}^{+\infty} \alpha_t [1 + \nabla_t(\alpha_t - a_t)] p(\alpha_t|Y_{t-1}) d\alpha_t \\ &= \int_{-\infty}^{+\infty} (a_t + \alpha_t - a_t) [1 + \nabla_t(\alpha_t - a_t)] p(\alpha_t|Y_{t-1}) d\alpha_t \\ &= \int_{-\infty}^{+\infty} [a_t + a_t \nabla_t(\alpha_t - a_t) + (\alpha_t - a_t) + \nabla_t(\alpha_t - a_t)^2] p(\alpha_t|Y_{t-1}) d\alpha_t \\ &= a_t + \nabla_t p_t \end{aligned}$$

where the terms in  $(\alpha_t - a_t)$  vanish after integrating over  $p(\alpha_t|Y_{t-1}) d\alpha_t$ .

We now consider the integral of the last term. Observe that we can write:

$$\int_{-\infty}^{+\infty} \alpha_t \frac{g(\alpha_t)}{p(y_t|\alpha_t)|_{a_t}} p(\alpha_t|Y_{t-1}) d\alpha_t \tag{B.1}$$

$$= \frac{1}{p(y_t|\alpha_t)|_{a_t}} \int_{-\infty}^{+\infty} (\alpha_t - a_t + a_t) g(\alpha_t) p(\alpha_t|Y_{t-1}) d\alpha_t \tag{B.2}$$

$$= \frac{1}{p(y_t|\alpha_t)|_{a_t}} \left[ \int_{-\infty}^{+\infty} (\alpha_t - a_t) g(\alpha_t) p(\alpha_t|Y_{t-1}) d\alpha_t + \int_{-\infty}^{+\infty} a_t g(\alpha_t) p(\alpha_t|Y_{t-1}) d\alpha_t \right] \tag{B.3}$$

The first integral in Eq. (B.3) can be decomposed as:

$$\begin{aligned} & \int_{-\infty}^{+\infty} (\alpha_t - a_t) g(\alpha_t) p(\alpha_t|Y_{t-1}) d\alpha_t = \int_{-\infty}^{a_t - \delta} (\alpha_t - a_t) g(\alpha_t) p(\alpha_t|Y_{t-1}) d\alpha_t \\ & + \int_{a_t - \delta}^{a_t + \delta} (\alpha_t - a_t) g(\alpha_t) p(\alpha_t|Y_{t-1}) d\alpha_t + \int_{a_t + \delta}^{+\infty} (\alpha_t - a_t) g(\alpha_t) p(\alpha_t|Y_{t-1}) d\alpha_t \end{aligned}$$



The integral over the neighborhood of center  $a_t$  and radius  $\delta$  can be bounded as follows:

$$\begin{aligned} \left| \int_{a_t-\delta}^{a_t+\delta} (\alpha_t - a_t)g(\alpha_t)p(\alpha_t|Y_{t-1})d\alpha_t \right| &\leq \int_{a_t-\delta}^{a_t+\delta} |\alpha_t - a_t||g(\alpha_t)|p(\alpha_t|Y_{t-1})d\alpha_t \\ &\leq M(\delta) \int_{a_t-\delta}^{a_t+\delta} |\alpha_t - a_t|^3 p(\alpha_t|Y_{t-1})d\alpha_t \\ &\leq M(\delta)\beta_t^{(3)} \end{aligned}$$

Now, let us consider the integral from  $a_t + \delta$  to  $+\infty$  and observe that we can write it as:

$$\begin{aligned} &\int_{a_t+\delta}^{+\infty} (\alpha_t - a_t)g(\alpha_t)p(\alpha_t|Y_{t-1})d\alpha_t \\ &= \int_{a_t+\delta}^{+\infty} (\alpha_t - a_t) \left[ p(y_t|\alpha_t) - p(y_t|\alpha_t)|_{a_t} - \frac{\partial p(y_t|\alpha_t)}{\partial \alpha_t} \Big|_{a_t} (\alpha_t - a_t) \right] p(\alpha_t|Y_{t-1})d\alpha_t \end{aligned}$$

We can bound this integral using the condition in Assumption 3, Lemma 1 and the boundedness of  $p(y_t|\alpha_t)$  in Assumption 1:

$$\begin{aligned} &\left| \int_{a_t+\delta}^{+\infty} (\alpha_t - a_t) \left[ p(y_t|\alpha_t) - p(y_t|\alpha_t)|_{a_t} - \frac{\partial p(y_t|\alpha_t)}{\partial \alpha_t} \Big|_{a_t} (\alpha_t - a_t) \right] p(\alpha_t|Y_{t-1})d\alpha_t \right| \\ &\leq \int_{a_t+\delta}^{+\infty} \frac{\sup_{\alpha_t > a_t+\delta} p(y_t|\alpha_t) + p(y_t|\alpha_t)|_{a_t}}{(\alpha_t - a_t)^{3+\beta}} d\alpha_t + \int_{a_t+\delta}^{+\infty} \frac{\left| \frac{\partial p(y_t|\alpha_t)}{\partial \alpha_t} \Big|_{a_t} \right|}{(\alpha_t - a_t)^{2+\beta}} d\alpha_t \\ &= \frac{1}{2+\beta} \frac{\sup_{\alpha_t > a_t+\delta} p(y_t|\alpha_t) + p(y_t|\alpha_t)|_{a_t}}{\delta^{2+\beta}} + \frac{1}{1+\beta} \frac{\left| \frac{\partial p(y_t|\alpha_t)}{\partial \alpha_t} \Big|_{a_t} \right|}{\delta^{1+\beta}} \end{aligned}$$

Similarly, the integral from  $-\infty$  to  $a_t$  can be bounded as follows:

$$\begin{aligned} &\left| \int_{a_t+\delta}^{+\infty} (\alpha_t - a_t) \left[ p(y_t|\alpha_t) - p(y_t|\alpha_t)|_{a_t} - \frac{\partial p(y_t|\alpha_t)}{\partial \alpha_t} \Big|_{a_t} (\alpha_t - a_t) \right] p(\alpha_t|Y_{t-1})d\alpha_t \right| \\ &\leq \frac{1}{2+\beta} \frac{\sup_{\alpha_t < a_t-\delta} p(y_t|\alpha_t) + p(y_t|\alpha_t)|_{a_t}}{\delta^{2+\beta}} + \frac{1}{1+\beta} \frac{\left| \frac{\partial p(y_t|\alpha_t)}{\partial \alpha_t} \Big|_{a_t} \right|}{\delta^{1+\beta}} \end{aligned}$$

Thus, we have:

$$\begin{aligned} &\left| \int_{-\infty}^{+\infty} (\alpha_t - a_t)g(\alpha_t)p(\alpha_t|Y_{t-1})d\alpha_t \right| \\ &\leq M(\delta)\beta_t^{(3)} + \frac{1}{2+\beta} \frac{\sup_{\alpha_t > a_t+\delta} p(y_t|\alpha_t) + \sup_{\alpha_t < a_t-\delta} p(y_t|\alpha_t) + 2p(y_t|\alpha_t)|_{a_t}}{\delta^{2+\beta}} + \frac{2}{1+\beta} \frac{\left| \frac{\partial p(y_t|\alpha_t)}{\partial \alpha_t} \Big|_{a_t} \right|}{\delta^{1+\beta}} \end{aligned}$$

We now need to bound the second integral in Eq. (B.3). As before, let us decompose it as:

$$\begin{aligned} &\int_{-\infty}^{+\infty} a_t g(\alpha_t) p(\alpha_t|Y_{t-1}) d\alpha_t = \int_{-\infty}^{a_t-\delta} a_t g(\alpha_t) p(\alpha_t|Y_{t-1}) d\alpha_t \\ &+ \int_{a_t-\delta}^{a_t+\delta} a_t g(\alpha_t) p(\alpha_t|Y_{t-1}) d\alpha_t + \int_{a_t+\delta}^{+\infty} a_t g(\alpha_t) p(\alpha_t|Y_{t-1}) d\alpha_t \end{aligned}$$

As in the previous step, these integrals can be bounded using Assumption 3, Lemma 1 and the boundedness of  $p(y_t|\alpha_t)$  in Assumption 1. Simple computations lead to:

$$\begin{aligned} & \left| \int_{-\infty}^{+\infty} a_t g(\alpha_t) p(\alpha_t | Y_{t-1}) d\alpha_t \right| \\ & \leq M(\delta) |a_t| p_t + \frac{|a_t|}{3 + \beta} \frac{\sup_{\alpha_t > a_t + \delta} p(y_t | \alpha_t) + \sup_{\alpha_t < a_t - \delta} p(y_t | \alpha_t) + 2p(y_t | \alpha_t)|_{a_t}}{\delta^{3+\beta}} + \frac{2|a_t|}{2 + \beta} \frac{\left| \frac{\partial p(y_t | \alpha_t)}{\partial \alpha_t} \right|_{a_t}}{\delta^{2+\beta}} \end{aligned}$$

Let us now choose  $\tilde{\delta}$  such that  $\tilde{\delta} > \max(\bar{\delta}, \delta^*)$ , where  $\delta^*$  is the lowest  $\delta$  satisfying the following inequality:

$$\begin{aligned} & \frac{1}{p(y_t | \alpha_t)|_{a_t}} \left[ \frac{1}{2 + \beta} \frac{\sup_{\alpha_t > a_t + \delta} p(y_t | \alpha_t) + \sup_{\alpha_t < a_t - \delta} p(y_t | \alpha_t) + 2p(y_t | \alpha_t)|_{a_t}}{\delta^{2+\beta}} + \frac{2}{1 + \beta} \frac{\left| \frac{\partial p(y_t | \alpha_t)}{\partial \alpha_t} \right|_{a_t}}{\delta^{1+\beta}} + \right. \\ & \left. + \frac{|a_t|}{3 + \beta} \frac{\sup_{\alpha_t > a_t + \delta} p(y_t | \alpha_t) + \sup_{\alpha_t < a_t - \delta} p(y_t | \alpha_t) + 2p(y_t | \alpha_t)|_{a_t}}{\delta^{3+\beta}} + \frac{2|a_t|}{2 + \beta} \frac{\left| \frac{\partial p(y_t | \alpha_t)}{\partial \alpha_t} \right|_{a_t}}{\delta^{2+\beta}} \right] < \gamma \end{aligned}$$

Setting  $\chi_t = \int_{-\infty}^{+\infty} \alpha_t \frac{g(\alpha_t)}{p(y_t | \alpha_t)|_{a_t}} p(\alpha_t | Y_{t-1}) d\alpha_t$ , we have that:

$$a_{t|t} = \frac{p(y_t | \alpha_t)|_{a_t}}{p(y_t | Y_{t-1})} [a_t + p_t \nabla_t + \chi_t]$$

where  $|\chi_t| < \gamma + \frac{1}{2p(y_t | \alpha_t)|_{a_t}} \sup_{|\alpha_t - a_t| < \tilde{\delta}} \left| \frac{\partial^2 p(y_t | \alpha_t)}{\partial \alpha_t^2} \right| \left( \beta_t^{(3)} + |a_t| p_t \right)$ .

Observe now that, since Assumption 3 implies Assumption 2, Proposition 1 holds and we can write:

$$\begin{aligned} a_{t|t} &= \frac{p(y_t | \alpha_t)|_{a_t}}{p(y_t | \alpha_t)|_{a_t} + \xi_t} (a_t + p_t \nabla_t + \chi_t) \\ &= a_t + p_t \nabla_t + \chi_t + \left( \frac{p(y_t | \alpha_t)|_{a_t}}{p(y_t | \alpha_t)|_{a_t} + \xi_t} - 1 \right) (a_t + p_t \nabla_t + \chi_t) \\ &= a_t + p_t \nabla_t + \chi_t + \left( -\frac{\xi_t}{p(y_t | \alpha_t)|_{a_t} + \xi_t} \right) (a_t + p_t \nabla_t + \chi_t) \\ &= a_t + p_t \nabla_t + \chi_t + O(\xi_t). \end{aligned}$$

□

## C Proof of Theorem 2

First, observe that:

$$p_{t|t} = \mathbb{E}[(\alpha_t - a_{t|t})^2 | Y_t] = \mathbb{E}[(\alpha_t - a_t)^2 | Y_t] - (a_{t|t} - a_t)^2 \quad (\text{C.1})$$

The first term can be written as:

$$\mathbb{E}[(\alpha_t - a_t)^2 | Y_t] = \int_{-\infty}^{+\infty} (\alpha_t - a_t)^2 \frac{p(y_t | \alpha_t) p(\alpha_t | Y_{t-1})}{p(y_t | Y_{t-1})} d\alpha_t$$

To compute this integral, we expand  $p(y_t|\alpha_t)$  at second order in a neighborhood of center  $a_t$  and radius  $\delta$ :

$$p(y_t|\alpha_t) = p(y_t|\alpha_t)|_{a_t} + \frac{\partial p(y_t|\alpha_t)}{\partial \alpha_t} \Big|_{a_t} (\alpha_t - a_t) + \frac{1}{2} \frac{\partial^2 p(y_t|\alpha_t)}{\partial \alpha_t^2} \Big|_{a_t} (\alpha_t - a_t)^2 + g(\alpha_t)$$

where  $|g(\alpha_t)| < M(\delta)|\alpha_t - a_t|^3$  for each  $\alpha_t$  belonging to the neighborhood. Thanks to Assumption 4, we have  $M(\delta) = \frac{1}{6} \sup_{|\alpha_t - a_t| < \delta} \left| \frac{\partial^3 p(y_t|\alpha_t)}{\partial \alpha_t^3} \right|$ . Moreover, we set  $\delta > \bar{\delta}$ , where  $\bar{\delta}$  is defined in Assumption 5. We can thus write:

$$\begin{aligned} \mathbb{E}[(\alpha_t - a_t)^2 | Y_t] &= \frac{p(y_t|\alpha_t)|_{a_t}}{p(y_t|Y_{t-1})} \int_{-\infty}^{+\infty} (\alpha_t - a_t)^2 [1 + \nabla_t (\alpha_t - a_t) + \\ &\quad + \frac{1}{2p(y_t|\alpha_t)|_{a_t}} \frac{\partial^2 p(y_t|\alpha_t)}{\partial \alpha_t^2} \Big|_{a_t} (\alpha_t - a_t)^2 + \frac{g(\alpha_t)}{p(y_t|\alpha_t)|_{a_t}}] p(\alpha_t|Y_{t-1}) d\alpha_t \end{aligned}$$

The integral of the first three terms results in:

$$\begin{aligned} &\int_{-\infty}^{+\infty} (\alpha_t - a_t)^2 \left[ 1 + \nabla_t (\alpha_t - a_t) + \frac{1}{2p(y_t|\alpha_t)|_{a_t}} \frac{\partial^2 p(y_t|\alpha_t)}{\partial \alpha_t^2} \Big|_{a_t} (\alpha_t - a_t)^2 \right] p(\alpha_t|Y_{t-1}) d\alpha_t \\ &= p_t + \nabla_t p_t^{(3)} + \frac{1}{2p(y_t|\alpha_t)|_{a_t}} \frac{\partial^2 p(y_t|\alpha_t)}{\partial \alpha_t^2} \Big|_{a_t} p_t^{(4)} \end{aligned}$$

where  $p_t^{(3)}$  and  $p_t^{(4)}$  denote the third and fourth moments of  $p(\alpha_t|Y_{t-1})$ , respectively. We can also write the previous expression as:

$$p_t + \frac{1}{p(y_t|\alpha_t)|_{a_t}} \frac{\partial^2 p(y_t|\alpha_t)}{\partial \alpha_t^2} \Big|_{a_t} p_t^2 + \ell_t \quad (\text{C.2})$$

where  $\ell_t = \nabla_t p_t^{(3)} + \frac{1}{2p(y_t|\alpha_t)|_{a_t}} \frac{\partial^2 p(y_t|\alpha_t)}{\partial \alpha_t^2} \Big|_{a_t} (p_t^{(4)} - 2p_t^2)$ . We now assess the second term in Eq. (C.1).

Observe that Proposition 1 and Theorem 1 hold under Assumptions 4, 5. Thus we can write:

$$\begin{aligned} (a_{t|t} - a_t)^2 &= \left[ \frac{p(y_t|\alpha_t)|_{a_t}}{p(y_t|Y_{t-1})} (a_t + p_t \nabla_t + \chi_t) - a_t \right]^2 \\ &= \left[ \left( \frac{p(y_t|\alpha_t)|_{a_t}}{p(y_t|Y_{t-1})} - 1 \right) a_t + \frac{p(y_t|\alpha_t)|_{a_t}}{p(y_t|Y_{t-1})} p_t \nabla_t + \frac{p(y_t|\alpha_t)|_{a_t}}{p(y_t|Y_{t-1})} \chi_t \right]^2 \\ &= \left[ -\frac{\xi_t}{p(y_t|\alpha_t)|_{a_t} + \xi_t} a_t + \frac{p(y_t|\alpha_t)|_{a_t}}{p(y_t|Y_{t-1})} p_t \nabla_t + \frac{p(y_t|\alpha_t)|_{a_t}}{p(y_t|Y_{t-1})} \chi_t \right]^2 \end{aligned}$$

The leading term in the above equation is the second one, whereas the first and the third terms are of order  $\xi_t$  and  $\chi_t$ , respectively. The square of the leading term can be written as:

$$\begin{aligned} &\left[ \frac{p(y_t|\alpha_t)|_{a_t}}{p(y_t|Y_{t-1})} \right]^2 (p_t)^2 (\nabla_t)^2 \\ &= \frac{p(y_t|\alpha_t)|_{a_t}}{p(y_t|Y_{t-1})} (p_t)^2 (\nabla_t)^2 \left[ \frac{p(y_t|\alpha_t)|_{a_t}}{p(y_t|Y_{t-1})} - 1 \right] + \frac{p(y_t|\alpha_t)|_{a_t}}{p(y_t|Y_{t-1})} (p_t)^2 (\nabla_t)^2 \\ &= -\frac{p(y_t|\alpha_t)|_{a_t}}{p(y_t|Y_{t-1})} (p_t)^2 (\nabla_t)^2 \frac{\xi_t}{p(y_t|Y_{t-1})} + \frac{p(y_t|\alpha_t)|_{a_t}}{p(y_t|Y_{t-1})} (p_t)^2 (\nabla_t)^2 \end{aligned}$$

Combining this result with Eq. (C.2), we can write  $p_{t|t}$  as:

$$p_{t|t} = \frac{p(y_t|\alpha_t)|_{a_t}}{p(y_t|Y_{t-1})} \left[ p_t + \frac{(p_t)^2}{p(y_t|\alpha_t)|_{a_t}} \frac{\partial^2 p(y_t|\alpha_t)}{\partial \alpha_t^2} \Big|_{a_t} - (p_t)^2 (\nabla_t)^2 + \ell_t \right] \\ + O(\xi_t) + O(\chi_t) + \frac{p(y_t|\alpha_t)|_{a_t}}{p(y_t|Y_{t-1})} \int_{-\infty}^{+\infty} (\alpha_t - a_t)^2 \frac{g(\alpha_t)}{p(y_t|\alpha_t)|_{a_t}} p(\alpha_t|Y_{t-1}) d\alpha_t$$

where  $O(\xi_t)$ ,  $O(\chi_t)$  denote higher order terms in  $\xi_t$  and  $\chi_t$ . Before computing the last integral, observe that:

$$\frac{1}{p(y_t|\alpha_t)|_{a_t}} \frac{\partial^2 p(y_t|\alpha_t)}{\partial \alpha_t^2} \Big|_{a_t} - (\nabla_t)^2 \\ = \frac{1}{p(y_t|\alpha_t)|_{a_t}} \frac{\partial^2 p(y_t|\alpha_t)}{\partial \alpha_t^2} \Big|_{a_t} - \left( \frac{1}{p(y_t|\alpha_t)|_{a_t}} \frac{\partial p(y_t|\alpha_t)}{\partial \alpha_t} \Big|_{a_t} \right)^2 \\ = \frac{\partial^2 \log p(y_t|\alpha_t)}{\partial \alpha_t^2} \Big|_{a_t}$$

The term in the last line is the Hessian of the log-density evaluated in  $a_t$ . Denoting this quantity by  $h_t$ , we can re-write  $p_{t|t}$  more compactly as:

$$p_{t|t} = \frac{p(y_t|\alpha_t)|_{a_t}}{p(y_t|Y_{t-1})} \left[ p_t + (p_t)^2 h_t + \ell_t \right] + O(\xi_t) + O(\chi_t) \\ + \frac{p(y_t|\alpha_t)|_{a_t}}{p(y_t|Y_{t-1})} \int_{-\infty}^{+\infty} (\alpha_t - a_t)^2 \frac{g(\alpha_t)}{p(y_t|\alpha_t)|_{a_t}} p(\alpha_t|Y_{t-1}) d\alpha_t$$

To conclude the proof, we need to bound the integral in  $g(\alpha_t)$ . Let us decompose this integral as<sup>10</sup>:

$$\int_{-\infty}^{+\infty} (\alpha_t - a_t)^2 g(\alpha_t) p(\alpha_t|Y_{t-1}) d\alpha_t = \int_{-\infty}^{a_t-\delta} (\alpha_t - a_t)^2 g(\alpha_t) p(\alpha_t|Y_{t-1}) d\alpha_t \\ + \int_{a_t-\delta}^{a_t+\delta} (\alpha_t - a_t)^2 g(\alpha_t) p(\alpha_t|Y_{t-1}) d\alpha_t + \int_{a_t+\delta}^{+\infty} (\alpha_t - a_t)^2 g(\alpha_t) p(\alpha_t|Y_{t-1}) d\alpha_t$$

The integral over the neighborhood of center  $a_t$  and radius  $\delta$  can be bounded thanks to Assumption 4:

$$\left| \int_{a_t-\delta}^{a_t+\delta} (\alpha_t - a_t)^2 g(\alpha_t) p(\alpha_t|Y_{t-1}) d\alpha_t \right| \leq \int_{a_t-\delta}^{a_t+\delta} (\alpha_t - a_t)^2 |g(\alpha_t)| p(\alpha_t|Y_{t-1}) d\alpha_t \\ = \int_{a_t-\delta}^{a_t+\delta} M(\delta) |\alpha_t - a_t|^5 p(\alpha_t|Y_{t-1}) d\alpha_t \\ \leq M(\delta) \beta_t^{(5)}$$

<sup>10</sup>Hereafter, we neglect the term  $\frac{1}{p(y_t|\alpha_t)_{a_t}}$ , which will be absorbed in the definition of  $\delta^*$  below.

The two integrals outside the neighborhood can instead be bounded using Assumption 5, Lemma 1 and the boundedness of  $p(y_t|\alpha_t)$  in Assumption 1. Let us focus first on the third integral:

$$\begin{aligned}
& \left| \int_{a_t+\delta}^{+\infty} (\alpha_t - a_t)^2 g(\alpha_t) p(\alpha_t|Y_{t-1}) d\alpha_t \right| \\
& \leq \int_{a_t+\delta}^{+\infty} (\alpha_t - a_t)^2 |g(\alpha_t)| p(\alpha_t|Y_{t-1}) d\alpha_t \\
& = \int_{a_t+\delta}^{+\infty} (\alpha_t - a_t)^2 \left| p(y_t|\alpha_t) - p(y_t|\alpha_t)|_{a_t} - \frac{\partial p(y_t|\alpha_t)}{\partial \alpha_t} \Big|_{a_t} (\alpha_t - a_t) \right. \\
& \quad \left. - \frac{1}{2} \frac{\partial^2 p(y_t|\alpha_t)}{\partial \alpha_t^2} \Big|_{a_t} (\alpha_t - a_t)^2 \right| p(\alpha_t|Y_{t-1}) d\alpha_t \\
& \leq \int_{a_t+\delta}^{+\infty} \frac{\sup_{\alpha_t > a_t+\delta} p(y_t|\alpha_t) + p(y_t|\alpha_t)|_{a_t}}{(\alpha_t - a_t)^{4+\beta}} d\alpha_t + \int_{a_t+\delta}^{+\infty} \frac{\left| \frac{\partial p(y_t|\alpha_t)}{\partial \alpha_t} \Big|_{a_t} \right|}{(\alpha_t - a_t)^{3+\beta}} d\alpha_t \\
& \quad + \int_{a_t+\delta}^{+\infty} \frac{\left| \frac{1}{2} \frac{\partial^2 p(y_t|\alpha_t)}{\partial \alpha_t^2} \Big|_{a_t} \right|}{(\alpha_t - a_t)^{2+\beta}} d\alpha_t \\
& = \frac{1}{3+\beta} \frac{\sup_{\alpha_t > a_t+\delta} p(y_t|\alpha_t) + p(y_t|\alpha_t)|_{a_t}}{\delta^{3+\beta}} + \frac{1}{2+\beta} \left| \frac{\partial p(y_t|\alpha_t)}{\partial \alpha_t} \Big|_{a_t} \right| \frac{1}{\delta^{2+\beta}} \\
& \quad + \frac{1}{1+\beta} \left| \frac{1}{2} \frac{\partial^2 p(y_t|\alpha_t)}{\partial \alpha_t^2} \Big|_{a_t} \right| \frac{1}{\delta^{1+\beta}}
\end{aligned}$$

The integral from  $-\infty$  to  $a_t$  can be bounded in a similar way. The proof proceeds as in Section B, i.e. by setting  $\tilde{\delta}$  such that  $\tilde{\delta} > \max(\bar{\delta}, \delta^*)$ , where  $\delta^*$  is the lowest value of  $\delta$  for which the sum of the two integrals outside the neighborhood of center  $a_t$  is in absolute value lower than  $\gamma$ . Setting  $\zeta_t = \int_{-\infty}^{+\infty} (\alpha_t - a_t)^2 \frac{g(\alpha_t) p(\alpha_t|Y_{t-1})}{p(y_t|\alpha_t)|_{a_t}} d\alpha_t$ , we thus have:

$$p_{t|t} = \frac{p(y_t|\alpha_t)|_{a_t}}{p(y_t|Y_{t-1})} \left[ p_t + (p_t)^2 h_t + \ell_t + \zeta_t \right] + O(\xi_t) + O(\chi_t)$$

where  $|\zeta_t| < \gamma + \frac{1}{6p(y_t|\alpha_t)|_{a_t}} \sup_{|\alpha_t - a_t| < \delta} \left| \frac{\partial^3 p(y_t|\alpha_t)}{\partial \alpha_t^3} \right| \beta_t^{(5)}$ . To conclude the proof, observe that if Assumptions 4 and 5 are satisfied, then Proposition 1 holds and we can write:

$$\begin{aligned}
p_{t|t} & = \frac{p(y_t|\alpha_t)|_{a_t}}{p(y_t|\alpha_t)|_{a_t} + \xi_t} \left[ p_t + (p_t)^2 h_t + \ell_t + \zeta_t \right] + O(\xi_t) + O(\chi_t) \\
& = p_t + (p_t)^2 h_t + \ell_t + \zeta_t - \frac{\xi_t}{p(y_t|\alpha_t)|_{a_t} + \xi_t} [p_t + (p_t)^2 h_t + \ell_t + \zeta_t] + O(\xi_t) + O(\chi_t) \\
& = p_t + (p_t)^2 h_t + \ell_t + \zeta_t + O(\xi_t) + O(\chi_t).
\end{aligned}$$

□

## D Approximate recursions under a generic normalization matrix

$\mathbf{S}_t$

In score-driven models, the normalization matrix  $\mathbf{S}_t$  in Eq. (2.38) does not coincide with the one used in the approximate filtering algorithm of Section (2.2). Typically,  $\mathbf{S}_t$  is set equal to  $\mathbf{I}_t^{-\alpha}$ , where  $\mathbf{I}_t$  is the conditional Fisher information matrix. Common choices for the exponent  $\alpha$  are 0,  $\frac{1}{2}$  or 1. As discussed in Section (2.4), in this case the conditional covariance matrix  $\mathbf{P}_t$  can be defined by analogy with Eq. (2.38), i.e. by setting  $\mathbf{P}_t = \mathbf{T}^{-1}\mathbf{A}\mathbf{S}_t$  and replacing such expression in the recursions of Section (2.2). With this choice, the approximate recursions become:

$$\begin{aligned} \mathbf{a}_{t|t} &= \mathbf{a}_t + \mathbf{P}_t \nabla_t & \mathbf{P}_{t|t} &= \mathbf{P}_t + \mathbf{P}_t \mathbf{H}_t \mathbf{P}_t \\ \mathbf{a}_{t+1} &= \mathbf{c} + \mathbf{T}\mathbf{a}_t + \mathbf{A}\mathbf{S}_t \nabla_t & \mathbf{P}_t &= \mathbf{T}^{-1}\mathbf{A}\mathbf{S}_t \end{aligned}$$

for  $t = 1, \dots, n$ , and

$$\begin{aligned} \mathbf{r}_{t-1} &= \nabla_t + \mathbf{T}(\mathbf{I} + \mathbf{P}_t \mathbf{H}_t) \mathbf{r}_t & \mathbf{N}_{t-1} &= -\mathbf{H}_t + (\mathbf{I} + \mathbf{P}_t \mathbf{H}_t)' \mathbf{T}' \mathbf{H}_t \mathbf{T} (\mathbf{I} + \mathbf{P}_t \mathbf{H}_t) \\ \hat{\boldsymbol{\alpha}}_t &= \mathbf{a}_t + \mathbf{P}_t \mathbf{r}_{t-1} & \hat{\mathbf{P}}_t &= \mathbf{P}_t - \mathbf{P}_t \mathbf{N}_{t-1} \mathbf{P}_t \end{aligned}$$

for  $t = n, \dots, 1$ . Since  $\mathbf{S}_t$  depends on the Fisher information matrix, the above expressions assume a simpler form if the Hessian matrix  $\mathbf{H}_t$  is replaced by  $\mathbf{I}_t$ . This choice usually does not affect significantly the performance of the algorithm, but may improve its numerical stability when state variables are very erratic.

## E The case with a scalar signal ( $p = 1$ ) and more latent components ( $m > 1$ )

Let  $y_t \in \mathbb{R}$ ,  $\mathbf{a}_t \in \mathbb{R}^m$ ,  $m > 1$  and  $\mathbf{Z} \in \mathbb{R}^{1 \times m}$ . Let us consider an observation density  $p(y_t | \theta_t)$ , where  $\theta_t = \mathbf{Z}\mathbf{a}_t$  is a scalar signal. The score is given by:

$$\nabla_t = \frac{\partial \log p(y_t | \theta_t)}{\partial \mathbf{a}_t} = \mathbf{Z}' \nabla_t^{(\theta_t)} \quad (\text{E.1})$$

where  $\nabla_t^{(\theta_t)} = \frac{\partial \log p(y_t | \theta_t)}{\partial \theta_t}$  is scalar. Similarly, the Fisher information matrix is given by:

$$\mathbf{I}_t = \text{E}_{t-1}[\nabla_t \nabla_t'] = \mathbf{Z}' \mathbf{Z} i_t^{(\theta_t)} \quad (\text{E.2})$$

where  $i_t^{(\theta_t)} = \text{E}_{t-1}[\nabla_t^{(\theta_t)2}]$  is scalar.

Let us consider the case in which  $\mathbf{a}_t$  evolves based on the score-driven scheme in Eq. (2.38):

$$\mathbf{a}_{t+1} = \mathbf{c} + \mathbf{T}\mathbf{a}_t + \mathbf{A}\nabla_t \quad (\text{E.3})$$

where, since  $\mathbf{I}_t$  is singular, we have set  $\mathbf{S}_t = \mathbf{I}$ . Such choice for the normalization is equivalent to imposing a steady-state solution for the model. The last term can be written as  $\mathbf{a}\nabla_t^{(\theta_t)}$ , where

$\mathbf{a} = \mathbf{AZ}'$ . It follows that we can only identify the vector  $\mathbf{a}$ , but not the full matrix  $\mathbf{A}$ . Similarly, since  $\mathbf{P}_t = \mathbf{T}^{-1}\mathbf{A}$ , we can only identify the vector  $\mathbf{P}_t\mathbf{Z}'$ , but not the full matrix  $\mathbf{P}_t$ . This is not an issue when computing the two filters in Eq. (2.18), (2.19), as they only depend on  $\mathbf{P}_t\mathbf{Z}'$ . In contrast, the smoother in Eq. (2.22), (2.23) depend on  $\mathbf{P}_t$  and thus we obtain different smoothed estimates depending on the choice of  $\mathbf{A}$  from the admissible set. The same argument can be generalized to the case  $p > 1$  and  $m > p$ . In such cases, the matrix  $\mathbf{P}_t$  is identifiable provided that one uses the normalization given by Eq. (2.21), which is analogous to that used in the standard Kalman filter.